Integrated design strategy for EU-DEMO first wall protection from plasma transients

Fusion Engineering and Design 177 (2022) 113067

Contents lists available at ScienceDirect

Fusion Engineering and Design

journal homepage: www.elsevier.com/locate/fusengdes

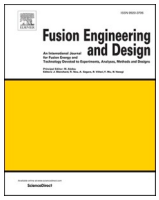

Integrated design strategy for EU-DEMO first wall protection from plasma transients

Francesco Maviglia [a,b,*], Christian Bachmann [a,n], Gianfranco Federici [a], Thomas Franke [a,c], Mattia Siccinio [a,c], Raffaele Albanese [d], Roberto Ambrosino [d], Wayne Arter [m], Roberto Bonifetto [e], Giuseppe Calabrò [f], Riccardo De Luca [f], Luigi E. Di Grazia [o], Emiliano Fable [c], Pierluigi Fanelli [f], Alessandra Fanni [g], Mehdi Firdaouss [h], Jonathan Gerardin [i], Riccardo Lombroni [f], Massimiliano Mattei [d], Matteo Moscheni [e], William Morris [m], Gabriella Pautasso [c], Sergey Pestchanyi [l], Giuseppe Ramogida [b], Maria Lorena Richiusa [m], Giuliana Sias [g], Fabio Subba [e], Fabio Villone [d], Jeong-Ha You [c], Zsolt Vizvary [m]

[a] *EUROfusion – Programme Management Unit, Boltzmannstrasse 2, 85748 Garching, Germany*
[b] *Associazione EURATOM-ENEA sulla Fusione, C.R. Frascati, C.P. 65-00044 Frascati, Rome, Italy*
[c] *Max-Planck-Institut für Plasmaphysik, Garching, Germany*
[d] *Consorzio CREATE, Univ. Napoli Federico II - DIETI, 80125 Napoli, Italy*
[e] *NEMO Group, Dip. Energia, Politecnico di Torino, C.so Duca degli Abruzzi24, Torino 10129, Italy*
[f] *DEIm Department, University of Tuscia, Largo dell'Universitá, 01100 Viterbo, Italy*
[g] *Electrical and Electronic Engin. Dept.-University of Cagliari, Piazza D'Armi, 09123, Cagliari, Italy*
[h] *CEA, F-13108 St Paul-Lez-Durance, France*
[i] *Institute of Plasma Physics, Czech Academy of Sciences, Prague, Czech Republic*
[l] *KIT, Hermann-von-Helmholtz-Platz 1, Eggenstein-Leopoldshafen, Germany*
[m] *CCFE, Culham Science Centre, Abingdon, Oxon, OX14 3DB, UK*
[n] *Technical University of Denmark, Lyngby, Denmark*
[o] *Consorzio CREATE, Univ. della Campania L. Vanvitelli, Dip. Ingegneria, 80131 Aversa, Italy*

ARTICLE INFO

Keywords:
DEMO
Plasma transients
First wall load
Electromagnetic simulations
Plasma scenario optimization
Discrete limiters

ABSTRACT

This work presents an overview of the integrated strategy developed, as part of the DEMO Key Design Integration Issue 1 (KDII1), to protect the EU-DEMO first wall (FW) from planned and unplanned plasma transients by employing discrete limiters. The present Breeding Blanket (BB) FW design, which aims at minimizing the loss of neutrons while travelling to the breeding zone, is able to withstand steady state heat fluxes up to ≈1-1.5 MW/m^2 [1], which is not sufficient to guarantee its integrity for most plasma-FW direct contact. This is different from ITER, which has a FW designed for peak heat loads up to 4.6 MW/m^2 [2], and it does not have the DEMO BB breeding related requirement. A series of documents was compiled in the DEMO Pre-Conceptual Design Phase, in support of the KDII1. The work presented here was presented at the 2020 DEMO Gate 1 (G1) review, and collects also the comments of the panel and the relative additional studies triggered by them. The design process, presented in this paper was adopted to systematically evaluate the impact of design changes, or new physics inputs, on the FW protection strategy and integration issues. It includes compiling the list of transients, and performing the relative plasma simulations, the design of discrete limiters and the evaluation of their capability to reduce the heat flux density on the FW, and finally a preliminary analysis of the heat loads effects on the Plasma Facing Components (PFC). All these aspects, together with preliminary limiter design, where considered since the beginning, in an integrated way.

* Corresponding author.

https://doi.org/10.1016/j.fusengdes.2022.113067
Received 3 August 2021; Received in revised form 23 December 2021; Accepted 15 February 2022
Available online 20 February 2022

1. Introduction

This paper presents an integrated design strategy for the first-wall (FW) protection from plasma normal and off-normal transients, which has been developed as one of the Key Design Integration Issues (KDIIs) [3] during the DEMO Pre-Concept Design (PCD) Phase. The issue of the FW protection is fundamentally different from the ITER one, hence its solution cannot be applied to DEMO. The present DEMO breeding blanket (BB) FW design is characterized by a steady state heat load upper limit of no more than ≈1-1.5 MW/m^2 [1], for both helium and water-cooled concepts. This constraint is due to the DEMO specific requirements to use high neutron irradiation resistant materials, such as EUROFER, to have high coolant temperature, for an efficient energy conversion, and to maximize the tritium breeding ratio (TBR) with a structure which is as transparent as possible to neutrons. In comparison the present ITER FW, which does not have a breeding blanket behind, is currently designed as whole "conforming wall" to sustain heat flux (HF) densities up to 4.6MW/m^2 [2]. This strategy has been also presented at the 2020 DEMO G1 review, which included the assessment of a number of variants for each KDII. Two variants of FW protections were studied, including: single null (SN) divertor configurations with bare first wall, and with protection limiters. This paper explores a particular DEMO design, presented in [4] in more detail. The intention is to establish a methodology and test if it works (or where it has shortcomings). The additional aim is to guide a first design optimization, and a first exploration of the resilience of the design to uncertainties in the plasma scenario. This provides both a framework for future design evolution, and it also highlights issues and techniques that need specific attention in the next Concept Design (CD) Phase Fig. 1. shows the steps of the design process developed for the FW protection strategy.

This paper is structured such as to present each of these blocks in a different section. Section 2 includes a collection of the physics parameters of nominal and off normal events considered. These scenarios are then used as input, in the following Section 3, to run electromagnetic simulations aimed at locating the poloidal position of plasma-FW impact. The resulting magnetic flux maps are used, in Section 4, to evaluate the HF on the design-dependent plasma facing components (PFC), due both to the charged particles and to the radiation loads, and including sensitivity studies on power e-folding length. The results are used, in Section 5, to give feedback for the design of the shape, protrusion, toroidal number and poloidal location of the protection limiters and the plasma scenarios, until a satisfactory solution is found for the protection of the FW. Sensitivity studies are also carried out on limiters surfaces misalignments and their effect on the maximum HF.

2. Plasma steady state and transient identification

This work was performed as an integrated part of the physics activities related to the plasma scenario selection of the DEMO PCD phase and, in particular, with [5, 6] in this special issue. The aim of this activity is to collect a list, as complete as possible, of all normal events and steady state plasma scenario, which are planned in advance for certain phases of a plasma discharge (e.g. plasma current ramp up/down), and off-normal events that may take place (e.g. plasma disruptions). The latter category is of particular concern for the design of DEMO, and a major target of the plasma scenario design is to minimize as much as possible those occurrences, due both to physics uncertainties and to technical failures, as described in [5, 6].

The current list of transients was generated using:

An initial list of events extracted from the ITER Heat and Nuclear Load Specification document [7].

DEMO synthetic data, coming from plasma transport simulation codes, such as ASTRA/Simulink [8] and SOLPS-ITER [9], including, for instance, impurities influx in the machine, or additional heating/fuelling systems technical failures.

An experimental inter-machine database covering data from several machines (i.e. JET, EAST, ASDEX), in the operational space relevant for DEMO, including, for the time being, Upward/Downward Vertical Displacement Events (U/D-VDE), Major (diverted) Disruptions (MD) H-L and L-H transitions, edge localized modes (ELMs) and minor disruptions.

The transients were characterised in term of internal parameter variations, i.e. plasma current (I_p) poloidal beta (β_{pol}) and plasma internal inductance (l_i) as shown in [10], which are then used to perform the open loop plasma electromagnetic simulations discussed in the next section. A fully consistent closed loop simulation, including strongly coupled magnetic and kinetic control, is currently being developed, and represents one of the main objective of the next Conceptual Design Phase. The list of the steady state and plasma transients considered in the current work can be found in [10] but it is re-written shortly hereafter for the sake of convenience, and it is accompanied by a simplified cartoon in Fig. 2.

This includes, for the normal events:

Start/End Of Flattop (SOF/EOF) – steady state; plasma current Ramp Up/Down (RU/RD).

For the off-normal events, the cases analyzed are:

Upward/Downward Vertical Displacement Events (U/D-VDEs),

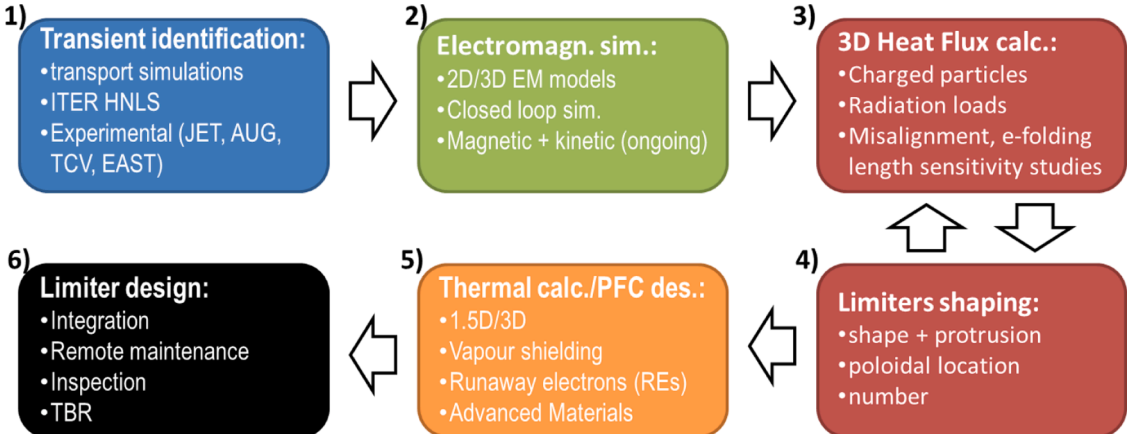

Fig. 1. Scheme of the developed process for the DEMO FW protection strategyThe resulting calculated HFs are used, in Section 6Section 6, to estimate the thermal behavior of possible PFC designs for a broad range of HF densities and deposition times, including possible mitigation effects coming from tungsten (W) vapor shielding. The 3D maps of surface HF are also used by other DEMO Work Packages (WP), e.g. the Breeding Blanket (WPBB), to carry out more detailed analyses. Finally, the engineering design, integration aspects and some preliminary consideration on the remote maintenance of the discrete limiters are evaluated in Section 2Section 7. It should be mentioned that the various phases were not developed in the sequential way as they are presented, but in an interlinked manner, including, for instance, the integration aspects from the very beginning.

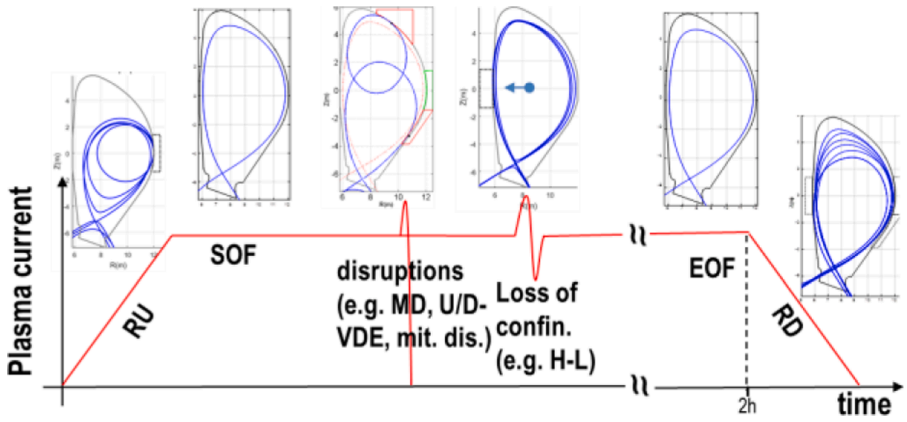

Fig. 2. Simplified representation of the DEMO normal (i.e. RU/RD, SOF/EOF) and off-normal (e.g. disruptions, loss of confinement) plasma phases considered in this work.

followed by an unmitigated disruption, with the plasma losing the vertical control and hitting the wall with the full thermal and magnetic energies, 1.3GJ and 1GJ respectively, as estimated in [11]. Different phases are considered, including plasma-wall first contact (First Touch), Thermal and Current Quenches (TQ and CQ) as described in [10]. The physics parameters of TQ and CQ are the same as the "Major (Centered) Disruptions", described below.

Mitigated disruptions, with the plasma energy being dissipated by photonic radiation following a deliberate injection of matter, as a mitigation action, as described in [10].

Controlled perturbations. Those represents perturbations, including ELMs and minor disruptions, as described in [10], which the plasma shape and vertical stability controls manage recover, avoiding the plasma-wall contact. The HF to the PFCs is evaluated at the time instant when the plasma boundary is closer to the wall.

Loss of plasma confinement. Those represents a list of perturbations evaluated by transport simulation carried out using ASTRA code, including influx of H_2O or W, missing pellets, failure of Neutral Beam Injection, etc. As for the case presented in [10], a conserve transient is here considered, i.e. a TQ on intermediate timescale, which cause the plasma wall contact on the inboard. This event is not linked to any identified transient, but is being used as a proxy to design a possible limiter in the inner wall.

Unmitigated Major (Centered) Disruptions (MD). This represent a newly considered transient, with respect to [10]. The physics parameters considered are similar to the unmitigated U/D-VDE, and which are repeated here for convenience:

Thermal Quench: (TQ). In this phase, all the thermal energy W_{th} (1.3GJ, as in [11]), or half of it (the other half being lost in the pre-TQ), is released in ≈1-4ms, while the plasma is still in diverted configuration, and it lands on the divertor, where severe damages are expected if no mitigation action is taken. During this transient, a broadening of the near SOL e-folding length of a factor ≈7 is considered (leading to λ_q≈7mm), similarly to ITER [7] where a broadening factor in the range =3-10 is used, and the plasma current is increased by 5-10%.

Current Quench (CQ): The final phase is represented by the CQ, during which the plasma current decrease from ~19MA to 0 in a time range, predicted for DEMO, from 74ms to 300ms, as described in [12]. The decay of the plasma current during the CQ is assumed to be linear and, conservatively, the 85% of the magnetic energy available to the plasma (W_{mag}≈1GJ) is supposed to be converted into energy carried by the charged particles, while the remaining 15% is radiated [13]. In this phase, two values of e-folding length are used, i.e. λ_q equal to 10mm (conservative) and 30mm (more realistic). This range is considered as it is very likely that during CQ the parameter λ_q became a function of time, which is not considered in this analysis, choosing instead the extreme of the ranges.

This list will be maintained and updated in the CD phase, as the project evolves and new knowledge is acquired, e.g. based on theoretical or experimental results of present or new machines, or design changes made for DEMO.

3. Electromagnetic model studies

During the PCD phase, several state-of-the-art codes have been used for the DEMO plasma magnetic equilibria and machine geometry optimization, and for the dynamic simulations. These are the 2D codes CREATE NL [14], MAXFEA [15] and PROTEUS [16], which have been benchmarked against each other and experimental data, and the 3D code CARMA0NL [17], and are presently used to plan and execute experiments in several devices. The latter has been used for analyses on the effects of non-toroidal axisymmetric electrically conductive structures (i.e. the BB segments, the vacuum vessel (VV) ports, and the divertor cassettes, see Fig. 3), being able to produce also 3D linearized models. These models have been used to tune the CREATE-NL 2D code, to take into account the equivalent dynamic 3D effects of passive structures on the radial and vertical field inside the vacuum chamber, in a range of frequencies of interest. Since 2D codes are computationally less expensive, CREATE-NL was used to simulate the wide range of plasma transients and configurations of interest. The proposed analyses is carried out, at present, without taking into account the ferromagnetic effects of the BB and of the ferromagnetic inserts used to minimize the toroidal field ripple. In addition MAXFEA 2D simulations have been used as input for a 3D ANSYS APDL model of the passive structures [18, 19], via a set of equivalent current filaments on a suitable grid simulating the effect of plasma (see Fig. 4). The transients listed in Section 2, with the relative internal plasma parameters variation, were used as an input to drive electromagnetic simulations, using the SN configuration from the DEMO baseline described in [20]. The aim was to simulate and save the magnetic flux maps in the standardized fusion EQDSK format [21], at the time instants of interest for plasma-wall interaction studies, e.g. when the plasma comes in contact with the FW, or it is closest to it. An example of the situations of interest is shown in Fig. 5.

During the PCD Phase, an optimization of the passive conductive structures, such as the BB and the vacuum vessel (VV), for vertical stability was carried out, bringing them as close as possible to the plasma. This also required an iteration on the FW shape [12].

Another activity involved the plasma shape optimization, by minimizing the distance between plasma current centroid and magnetic axis, which led as a consequence the plasma to be closer to the neutral point [22]. This increased the decoupling between the plasma vertical unstable mode with respect to the perturbations, hence reducing the vertical plasma movements following these disturbances [23]. Both these actions resulted in a significant improvement of vertical stabilization

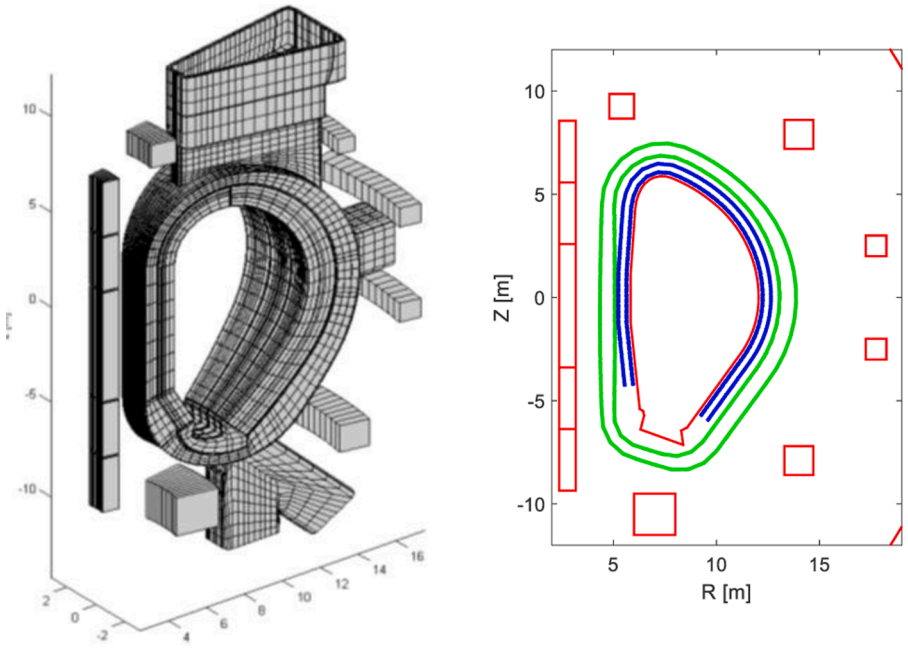

Fig. 3. Comparison of the 3D CARMA0NL model (on the left) including non-axisymmetric BB, and VV ports, with the equivalent 2D model (on the right) which includes additional conductive structures (in green and blue) tuned to best fit the dynamic behavior of the former in a frequency range of interest.

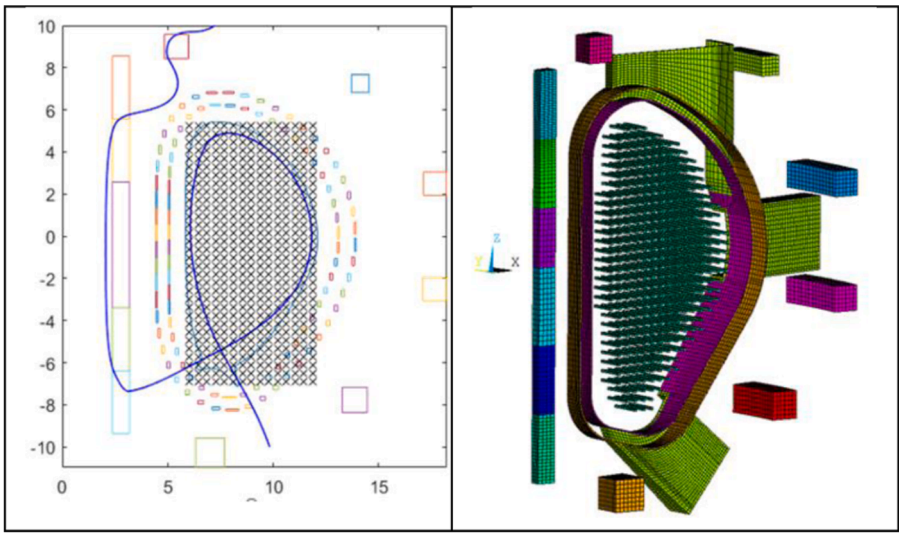

Fig. 4. Example of workflow for the forward coupling of 2D MAXFEA simulation to evaluate its effect on 3D conductive structures carried out in ANSYS APDL code.

(VS) overall performance, increasing the capability of the system to avoid U/D-VDE.

Finally, in [12], a methodology has been used to predict the plasma final position after the CQ, following a disruptive event, on the basis of the actual nominal magnetic flux-map. This approach aims to optimize the plasma equilibria, trying to bring the disruption damage locations close to maintenance ports already present in the machine (see Fig. 5, for an optimized Upward-VDE location), and tentatively design the protection limiters poloidal locations and extension.

3.1. Electromagnetic simulations of SN configurations transients and steady states phases

The simulations were carried out in collaboration with several EU-DEMO WPs, whose activities are also described in this special issue of Fusion Engineering and Design, i.e.:

Diagnostics and Control (WPDC), which helped to provided realistic controllers, and suggested diagnostics characterization;

Magnets (WPMAG) with whom PF coils maximum currents/voltages and changing rates were agreed;

Balance Of Plant (WPBOP) which provided simplified power supply transfer functions.

The electromagnetic simulations shown in Fig. 5 for the SN configuration were used to locate discrete protection limiters in four poloidal positions, shown in the Fig. 6, namely:

Outboard Mid-plane Limiters (OMLs), designed for the normal plasma ramp up and down phases.

Upper Limiters (ULs), designed for the off normal U-VDE events.

Outboard Lower Limiters (OLLs), designed for the off normal D-VDE events.

Inboard Mid-plane Limiters (IMLs), designed for off normal transition events characterized by a sudden loss of the plasma confinement

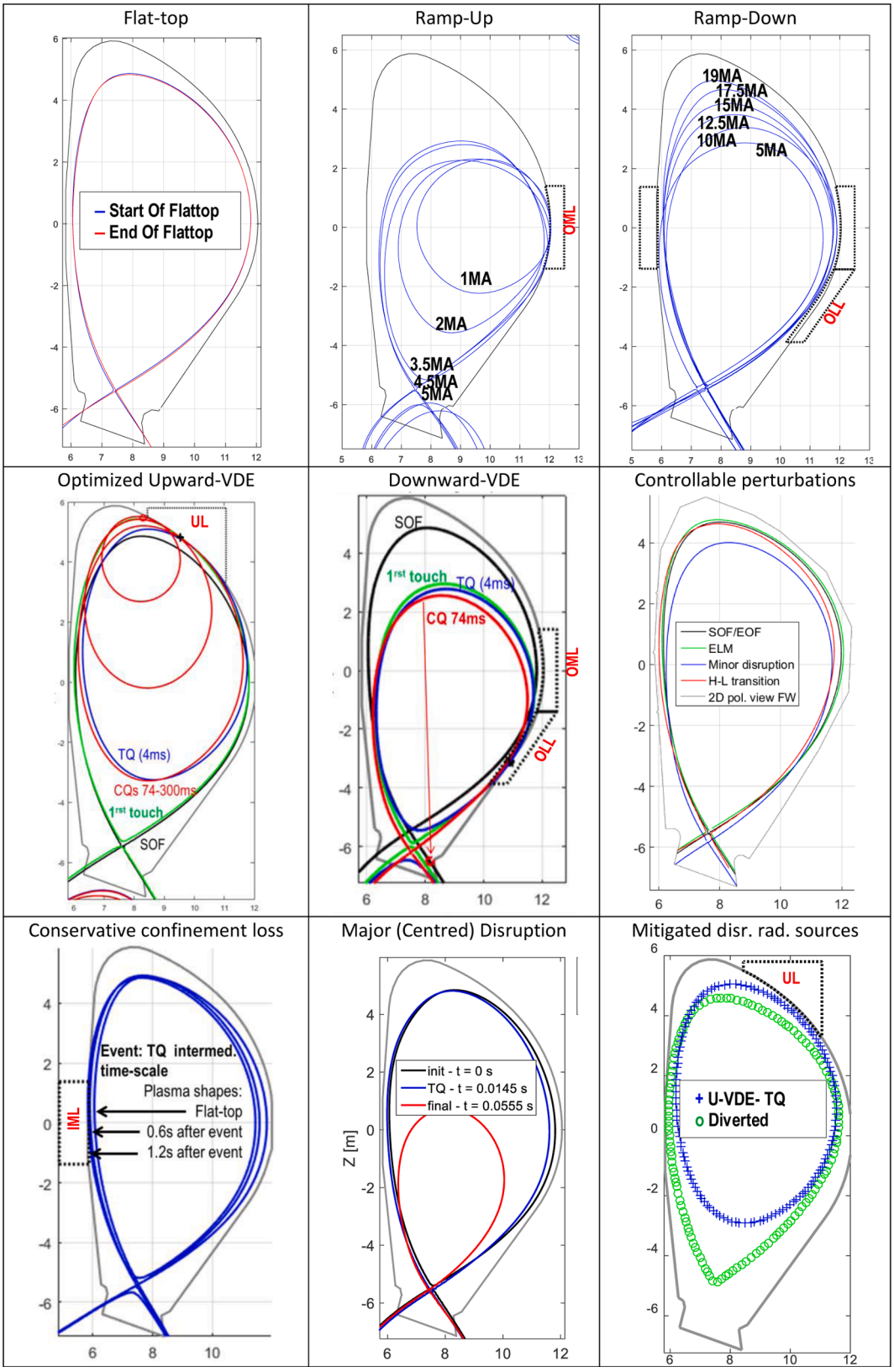

Fig. 5. Collection of magnetic equilibria of the normal events and off-normal transients described in [10]. For the transients, the phases before and after the plasma-FW contact (if any) and the possible limiters involved are shown. For disruptions (U/D-VDE and MD) also TQ/CQ phases are indicated, while for the mitigated disruptions the two sources considered to evaluate the photonic radiation loads, in case of limited configuration following a VDE, and diverted one, are shown.

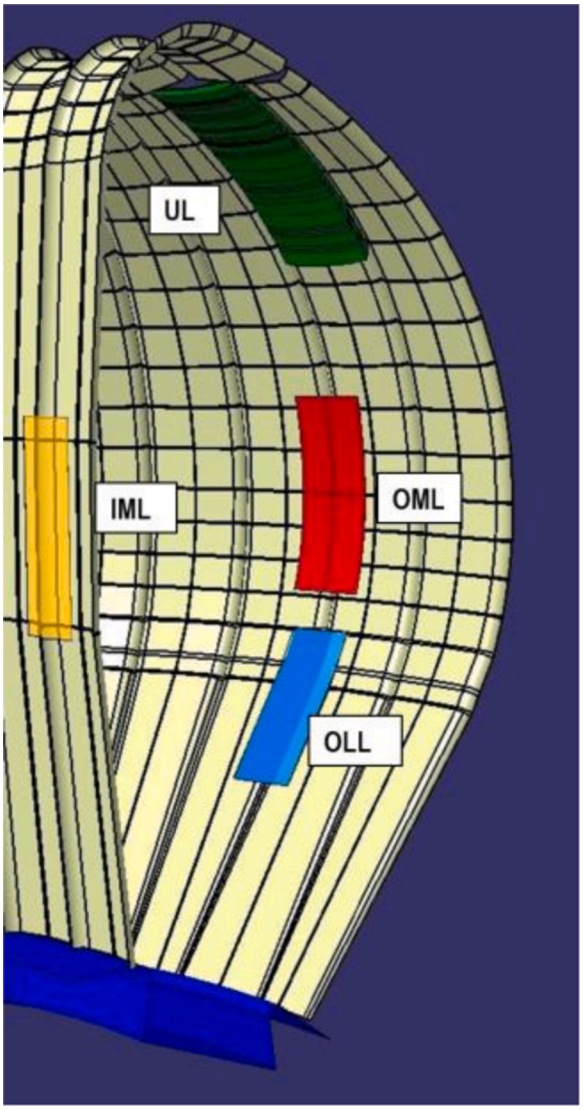

Fig. 6. Considered discrete limiter surfaces and poloidal locations, based on present DEMO transient simulations results.

energy, e.g. unplanned H-L transition, impurity event, and others as described in Section 2, leading to an inward movement.

The toroidal and poloidal extent of the OMLs and ULs are at present restricted by the maximum extent of the outboard equatorial port, described in [24], and the available space in the upper vertical port, described in [25]. The IMLs size is presently constrained also by the outboard equatorial port, from which a frontal maintenance scheme is under development, and described in [26]. Finally, the recently added OLLs are presently being developed and are thought to be maintained also by the equatorial ports.

4. 3D heat flux calculations

The outputs produced by the electromagnetic simulations, for the full list of plasma steady state and transient [20], were used as input for the HF calculations on the FW and all the PFCs. This process is done iteratively by evaluating the HF, and giving a feedback to the scenario and machine geometry optimization, by using a complete 3D FW design and 3D HF loads calculation.

The main source of heat loads considered in these documents are:

(Photonic) Radiative heat loads.

Thermal charged particles.

As mentioned in [20], this work does not include heat loads due to prompt fast particles losses, i.e. neutral beam injection and fusion alphas, as all investigations carried out within the EU-DEMO team on this topic have shown that their contribution is quite small. Also, the loads due to fusion neutrons, representing more a volumetric load, hence not affecting as strongly the PFC, is dealt with in [27]. Finally, as reported in [20], the interplay with Toroidal, and Beta-induced Alfvén Eigenmodes (TAEs, BAEs) and other MHD modes triggered by fast particles is not believed to be an issue in this respect, since these modes may affect the efficiency of the core plasma heating by redistributing alphas, but not the associated loads on PFCs, by virtue of the large size of the device. No conclusive studies are available on this latter point though, because of the high sensitivity of these modes on the core kinetic profiles, which at the moment are not robustly established.

For the radiative heat loads, an introduction to the role of radiation in DEMO can be found in [11, 20]. The Monte Carlo 3D CHERAB code [28] was employed to calculate the radiative HF. The simulation input consists of the radiation source calculated by the ASTRA [8] code, for the core, and by the SOLPS-ITER code [9] in a DEMO detached scenario, for the SOL. The thermal charged particle loads are calculated using the 3D field-line tracing codes PFCflux [29] and SMARDDA [30], which take as input the plasma magnetic equilibria, the assumptions on power density crossing the separatrix (Psol) and the e-folding length for the different power channels of the near and far scrape off layer ($\lambda_{q\_near\text{-}SOL}$, and $\lambda_{q\_far\text{-}SOL}$) presented in [10]. One of the issues encountered while evaluating this heat load contribution is that the field line tracing codes, like the one mentioned, model the heat load assuming that particles follow the magnetic field lines. This is conservative, as heat diffusion and turbulence phenomena will, to some extent, smooth the peak loads and lead to broader heat deposition profiles across magnetic flux tubes. In addition, calculations on limiter equilibria, and with a small discrete number of limiters, underestimate the heat load significantly as not all the power circulating in the SOL is mapped on the wall [31]. In the most problematic cases, the total power, calculated by evaluating the integral of the HF densities on the PFC surfaces, can represent only 10% of the one used as input, resulting on 90% of missing power. In ITER [32] this problem is less relevant, due to the fact that the first wall design does not include discrete limiters, as the whole FW acts as a limiter. The missing power issue is explained in detail in [31], where several approaches have been described on how to account for it. The approach used at present in the DEMO design, and presented in this paper, is to scale up the total power, evaluated by taking the integral of the HF densities on the PFC surface, such as to recover the original injected power. Previous ITER studies [33], on a less recent design which included two toroidal equally spaced limiters, have shown that adding a perpendicular transport heat flux term, parallel to the magnetic field lines considered by the PFCflux and SMARDDA codes, does not give rise to significant localised power loads. As the DEMO solution presented in this work uses a larger number of limiters, four instead of the two of the less recent ITER design [33], and being the uncertainty on the missing power lower with a larger number of limiters, also for DEMO we do not expect significant localised power loads. This analysis will be nevertheless reviewed in the next phase, by adding a perpendicular HF transport term, in line to what was done for ITER [33]. For every radiation and charged particles power deposition calculation, a series of information and data regarding the inputs and the resulting outputs are produced, catalogued (e.g. see Table 1) and made available for the engineering design of DEMO PFC, i.e.:

The CAD design of the 3D PFC surfaces.

The magnetic configuration of the plasma.

Plots showing the main components impacted by the particles and photons and corresponding 3D HF density data stored in the open source VTK file format VTK files [34].

A summary table containing, at a glance for all the cases, the input assumptions P_{sol}, the deposition time (for the transients), and the values for $\lambda_{q\_near/far\text{-}SOL}$.

Table 1
Summary of all the plasma steady state and transient cases analyzed. The results, in the Output columns, show the HF due to charged particles (in MW/m2, while in bold are indicated in GW/m2), evaluated with 3D field-line tracing codes (except the mitigated disruption where, instead, the photonic radiation, including toroidal and poloidal peaking factors, is reported). For the SOF and EOF are indicated in brackets, in italic, the HF including the radiation. *represents a D-VDE with the plasma shifted downwards (conservative). A subset of critical cases, in the output columns, is indicated with a superscript number within brackets

Inputs (Italic): with radiation, Bold: GW/m^2	Outputs: max HF (MW/m^2)								
Scenario	Case	P_{SOL} (MW)							
+(P_{RAD})	λ_q (mm)	Deposition time	OML	UL	OLL	IML	FW		
SOF	Diverted	69							
+(300 core + 130 SOL)	50	Steady state	0.53						
(0.65)	0.82								
(1.10)	0.09								
(0.33)	0								
(0.19)	0.40								
(0.59)									
EOF	Diverted	69							
+(300 core + 130 SOL)	50	Steady state	0.54						
(0.74)	1.25								
(1.42)	0.1								
(0.36)	0.9								
(1.11)	0.48								
(0.67)									
Min disr	Diverted	69	50	15-50ms	<0.01	0.13	0.01	3.06	0.69
ELM	Diverted	69	50	15-50ms	1.40	0.56	0	0	1.48
Ramp-Up	Limited	3.5	6	17.5-35s	2.37	0	0	0	0.29
Ramp-Down	Limited	5	6	25-50s	<0.01	<0.01	<0.01	0.02	0.01
		5	50	25-50s	<0.01	<0.01	<0.01	1.39	0.60
U-VDE	First touch	69	1	20-35ms	<0.01	114[2]	<0.01	0	0
		69	5	20-35ms	<0.01	15.6	<0.01	0	0.02
	TQ	$325\cdot10^3$	7	1-4ms	<0.01	63[3]	0	<0.01	138[8]
	Current Quench	10	10	74-200ms	<0.01	2.52	0	<0.01	0.01
		10	30	74-200ms	<0.01	1.53	0	<0.01	0.11
D-VDE	First touch	10 (*69)	10 (*1)	15-35ms	<0.01				
(*0.01)	0								
(*0)	<0.01								
(*24.8)	<0.01								
(*<0.01)	<0.01								
(*<0.01)									
		10 (*69)	30 (*5)	15-35ms	<0.01				
(*0.01)	0								
(*0)	<0.01								
(*7.83)	<0.01								
(*<0.01)	0.08								
(*0.01)									
	TQ	$325\cdot10^3$	7	1-4ms	0.77				
(*182)[1]	0								
(*0)	4.4								
(*306[4])	0.84								
(*11.3)	8.11								
(*292[9])									
	Current quench	10	10	74-200ms	<0.01	<0.01	<0.01	<0.01	<0.01
		10	30	74-200ms	<0.01	<0.01	<0.01	<0.01	<0.01
H-L transition	Limited (inboard)	30	2	1-5s	<0.01	<0.01	<0.01	64[5]	1.06
		30	4	1-5s	<0.01	<0.01	<0.01	44.5[6]	5.48
Major Disruption (MD)	TQ	$325\cdot10^3$	7	1-4ms	0.61	1.46	0.84	1.44[7]	333[10]
	CQ	10	10	74-200ms	<0.01	<0.01	<0.01	0.01	<0.01
		10	30	74-200ms	<0.01	<0.01	<0.01	0.21	0.05
Mitig.disr.	TQ	P_{RAD}.: 2.2 GW	1ms	2[11]	1.8[11]	1.8	1.5	2[11]	

The resulting maximum heat load for each of the discrete limiters and the FW.

4.1. E-folding length sensitivity studies

Sensitivity studies have been performed on the physics uncertainties present in the assumptions exploited, such as power e-folding length. This is particularly important because while for other parameters we have assumed initial conservative assumptions (e.g. by using the upper end of the ranges of plasma energy content that can be released during the disruptions, or the power crossing the separatrix), both a positive and negative variation of the λ_q parameter, with respect to the design value, will degrade the performance of the limiter. One of the most relevant planned transient is represented by the plasma current ramp-up phase, which will happen at every new discharge. The current estimate for the DEMO e-folding length in this phase is of λ_q=6mm [11], for a ramp up happening on the outer part of the vacuum chamber. The uncertainty range, as reported in [11], includes an e-folding length from 6mm to 9mm, based on [35], with 6mm being the smallest value, hence conservative, from the limiter point of view. The toroidal shape of the limiter is hence designed to spread as uniformly as possible the 6mm exponential power decay, as described in [26]. This is based on the approach described in [36].

A list of HF calculations has been assembled with the field line tracing codes, to evaluate the uncertainty on the e-folding length, with a variation of plasma e-folding length, $\lambda_{q,pla}$,from 4mm to 9mm. The results reported in Fig. 7. This calculation was carried out using 4 OMP limiters (the rationale for this number is explained in Section 5.1), equally toroidally spaced, i.e. at every 90 degrees Figs. 7. and 8 show that the limiter design experiences the lowest peak HF value for

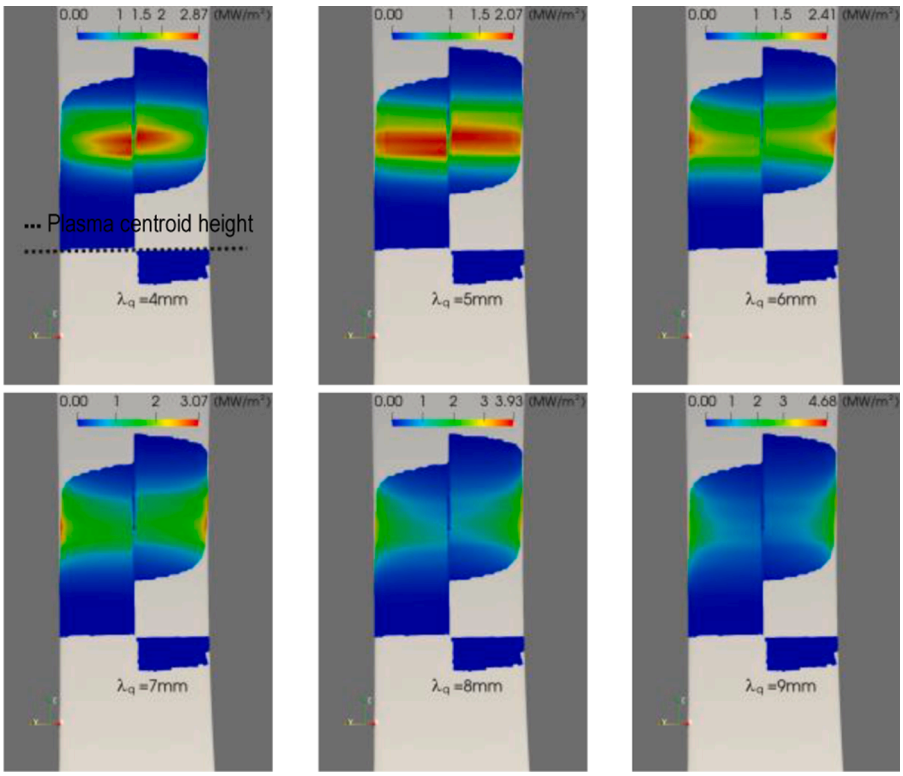

Fig. 7. Peak HF on OML, evaluated for a sensitivity scan of the for λ_q parameter from 4 mm to 9 mm, with 6 mm being the limiter design value. The dotted line represents the plasma centroid height, where the e-folding length is defined.

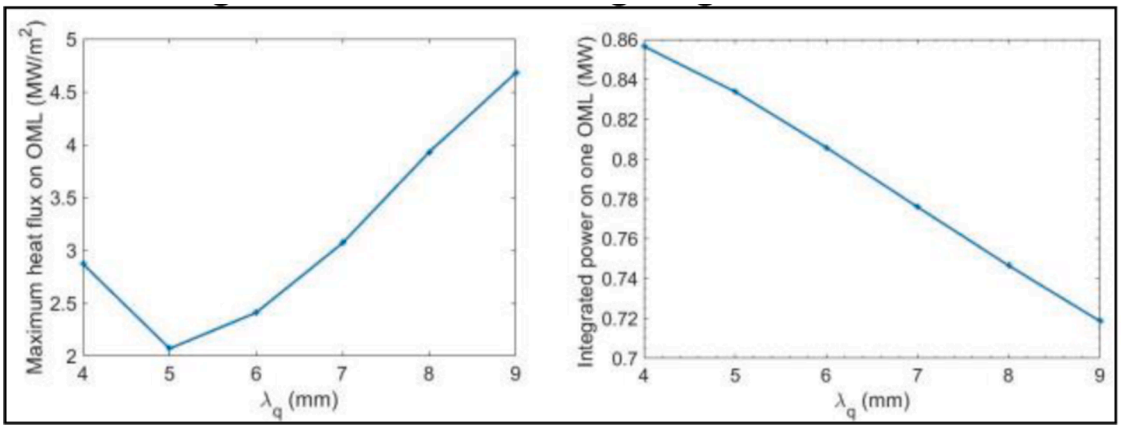

Fig. 8. Maximum HF density, and integrated power on an OML in function of the plasma λ_q sensitivity scan.

λ_q=5mm, and not the limiter design value of $\lambda_{q,lim}$ = 6mm.This is because the plasma-wall touching point it is at a different height with respect to the plasma centroid, and it has a magnetic flux expansion equal to 1.172, evaluates as:

$$f_{x,lim} = \frac{R_{pla}\ B_{pol,pla}}{R_{lim}\ B_{pol,lim}} \quad (1)$$

where R_{pla} and R_{lim} represents the radial coordinate, respectively, of the outer boundary of plasma centroid (where the e-folding length is defined, as shown in the dotted line of the top left Fig. 7) and of the plasma-limiter contact point, and B_{pol} the respective poloidal magnetic fields. Combining the limiter design value and the used plasma e-folding length with the flux expansion we obtain $\lambda_{q,lim} = \lambda_{q,plasma} / f_x = 5.12$mm, being the input plasma value for which the HF would spread uniformly, compatible with the results shown in Figs. 7 and 8. In Fig. 8 it is shown that below 5mm the maximum HF value is located in the centre of the OML, while for higher values the peak moves towards the sides of the OML reaching a bigger value due to higher incident angle. The integrated power on the limiter decreases when λ_q increases. This is because the magnetic field lines which are farther away from the plasma carry more energy when the λ_q increases so they can deposit more power on the FW. Giving the uncertainties on the physics inputs, and in the vertical plasma position during RU, leading to possible contact points with a slightly different flux expansion, hence effective e-folding length, it is important to design and test the robustness of the limiters for a as broad as possible range of λ_q, around the predicted one.

5. First wall and limiter shaping

A preliminary 3D model of the EU-DEMO limiters and the FW has

been developed within the work presented in this paper. The technical details of this design are reported in [26].

The first main element is represented by the BB FW, which was shaped to deal mainly with the steady state HF coming from the normal plasma phases, such as SOF and EOF. In this phase, the DEMO plasma scenario is designed to leave a clearance of at least 22.5cm from the plasma boundary to the PFC at the outer and inner mid-plane. In the other poloidal locations, a procedure was developed in [37] to automatically create a 2D FW poloidal profile such as to keep the resulting HF density on the PFCs surface below a prescribed value. This procedure uses as input the total power crossing the plasma separatrix, Psol, and the e-folding length relative to the far SOL, i.e. $\lambda_{q\ far_SOL} = 5$cm, as described in [20]. This initial 2D profile was used as guideline to develop the 3D FW shape, as described in [36].

The second element is represented by discrete limiters, which protrude from the FW towards the plasma. Their 3D surface is designed to: protect the FW armor from melting during the transients by keeping its HF density, under all considered circumstances, below its (steady state) technological limit $\approx$ 1-1.5MW/m^2 [1]. Possible higher HF transient cases, but fast, are analyzed case-by-case via thermal simulations; prevent the limiter cooling system from failing via appropriate design of its armor; spread as evenly as possible the power they receive, with the relative e-folding length, expected from the transient events predicted in their specific poloidal location; minimize the limiters number and size, to have the smallest possible impact on tritium breeding function performed by the BB, and reduce cost/complexity.

In order to be able to develop a remote handling strategy, the limiters toroidal and poloidal surface maximum extension is limited by the ports sizes, and the limiters should be ideally be placed close to the already planned maintenance ports.

Within these boundary conditions, several optimization activities were performed to evaluate the limiters shape, poloidal location and protrusion, in order to achieve the FW protection, by running the 3D HF calculations, described in Section 4, and using the results to feedback the design of their 3D shape.

5.1. Impact of the number of limiters to protect DEMO FW

Several studies have been made in the past [38] to estimate the minimum number of UL and OML needed to protect DEMO First Wall (FW). These studies allowed to have an initial guess on the minimum number of limiters for the present configuration, presented in the following sub sections. The most recent studies are based on EU-DEMO 2017 Baseline [4], which has 16 Toroidal field (TF) coils, hence BB sectors, hence a number of integer submultiples of limiters was analyzed, to allow an even toroidal spacing.

5.1.1. Number of OMLs

Studies were performed on the plasma current RU scenario evaluating 2 or 4 OMLs, as submultiple of the 16 TF coils, with a protrusion towards the plasma, with respect to the FW, of at least 2 cm [26]. 3D field-line tracing calculations were performed, using PFCflux and SMARDDA codes, using as input the power crossing the separatrix during the limiter phases:

5.1.2. Psol(MW) $\leq$ Plasma current(MA), as in [39]

and the near SOL e-folding length (λ_q) for the outboard limiter configuration is $\approx$ 6mm [11]. The worst case was used for the purpose of this study, i.e. Psol(MW) equal to Plasma current(MA). The results, as shown in Fig. 9, show that with 4 OMLs, the FW is well protected, experiencing a peak HF of 0.3MW/m^2, with moderate HF on OML (2.3 MW/m^2), which could be handled with a divertor W-mono block like technology [40], as discussed in paragraph 6. These values are obtained by multiplying the heat loads calculated by the codes by the power ratio factor = 0.4, which account for the issue of the missing power, discussed in the Section 4, and in detail in [31]. With the use of only two OMLs (one every 180°), the FW appears to be still protected with an estimated HF of 0.6MW/m^2, which is closer to the technological limit of 1-1.5 MW/m^2 [1]. In this case, the OMLs experience a HF of 4.3MW/m^2, which would still be within a "divertor like" W monoblock solution. However, the missing power issue becomes more severe with smaller number of limiters, with the power ratio down to 0.22, increasing the uncertainties of the HF calculation. For this reason, and to keep a margin

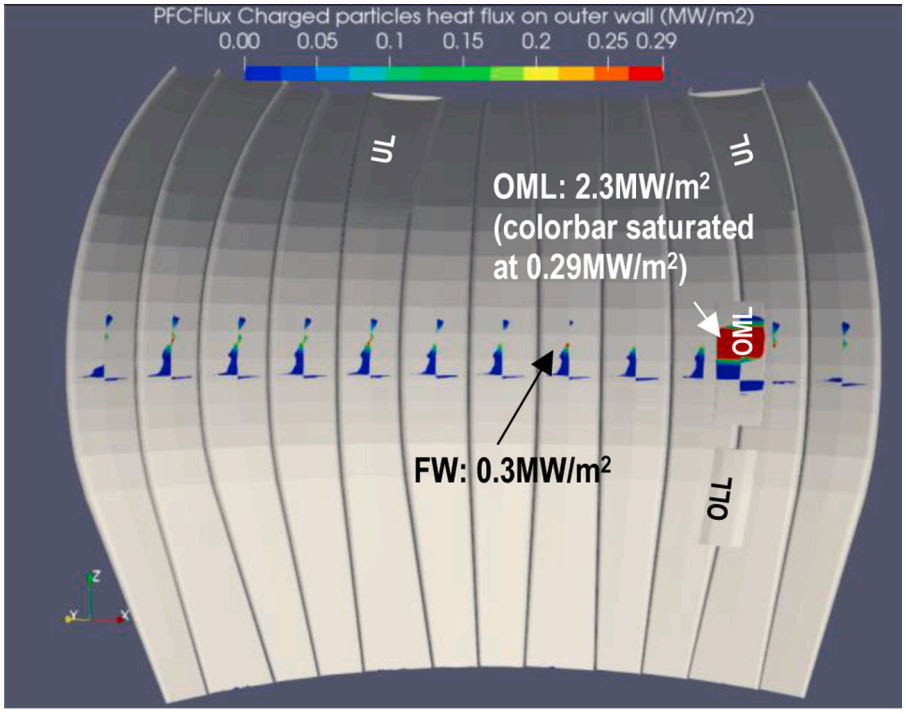

Fig. 9. HF on FW and OML, during RU with 4 OMLs (after rescaling the missing power).

on the FW and OML HF capability, it was decided for the time being to consider four as the minimum number of limiters. This decision might be revised in the CD Phase, if new reliable outcomes will be available, for instance, from the application of the method used in [33].

5.1.3. Number of ULs

For the ULs optimization, the unmitigated TQ, following a U-VDE, is considered with the following parameters:

Released = 1.3GJ [11], i.e. (conservatively) all the plasma kinetic energy at flat-top

Deposition time = 4ms, (the combination of point 1) and 2) leading to leading to a Psol=325GW, e-folding length considered was λ_q=7mm [10].

The sensitivity scan on the number of limiters was performed using 8 and 4 ULs, with a protrusion towards the plasma, with respect to the FW, of at least 7cm. This is due to the larger poloidal opening of the magnetic flux lines with respect to the outer mid-plane. The results were an increase of HF and wetted area on the FW, from 138MW/m^2 for 8ULs, to 408MW/m^2 for 4ULs.

While those values are quite high, they are both present for very short time, up to 4ms. The effects of these HF are evaluated in the Section 6, where the results of the performed thermal calculations are discussed. The issue of missing power ratio also increased drastically with the lower number of limiters (0.44 for 8ULs and 0.22 for 4ULs), increasing yet again the uncertainties. For those reasons it was decided to fix the ULs number to 8, as shown in Fig. 10. Moreover, no studies were made on toroidally asymmetric VDE (A-VDE) in the PCD Phase. This may be revised in the next phase, when, in case of asymmetric A-VDE, a smaller number of limiters could represent an even bigger problem for the protection of the FW. It is worth noticing that, for this conservative unmitigated TQ, the calculated peak HF on the UL is 64GW/m^2, which is orders of magnitude above the technological melting limits of the armor. Nonetheless the FW is still protected. The preliminary thermal calculation for limiters and FW will be discussed in the Section 6.

5.1.4. Scoping study of number of IMLs and OLLs

Similar calculations were also performed to evaluate the impact of the number and shape of the IML and OLL, respectively during the "Loss of energy confinement" and D-VDE transients. The latter two limiters have been developed more recently, and do not have the same level of detail of OMLs and ULs. The possibility to remotely maintaining the IML and OML via the equatorial port was preliminary assessed. As 4 OMLs are preliminarily allocated, it was decided to keep the maximum number of IML and OLL equal (or lower) to four. This preliminary simplistic assumption, which would allow a direct access to the back of each of the OLL, and a direct frontal access to the IMLs, as mentioned in [26], may be revised in the future in case a different number of limiters will be required.

The 3D HF calculations for each of the transients confirmed that four IMLs and OLLs would lead to a satisfactory protection of the FW also in those cases. As both OLLs and IMLs are not placed directly behind one of the planned maintenance ports, it is essential to verify their absolute need, by removing the conservative assumptions described above, as their absence will greatly simplify the in-vessel PFC systems design and maintenance.

5.1.5. Heat flux calculation on Single Null configuration with the proposed protection limiters

The presented optimization of the limiters leads to the following minimum number of them: 8 ULs, and 4 OMLs, OLLs and IMLs. In Fig. 11 examples of the HF calculations for the steady state and all the most severe phases of the transients are presented. Note that the RU and the U-VDE TQ are excluded as they are already shown in Figs. 9 and 10.

It is worth noticing that:

At present, for the TQ following a D-VDE, the plasma does not come in direct contact with the OLLs, but it is in a diverted configuration, engaging more directly the divertor system. This may not be the case for

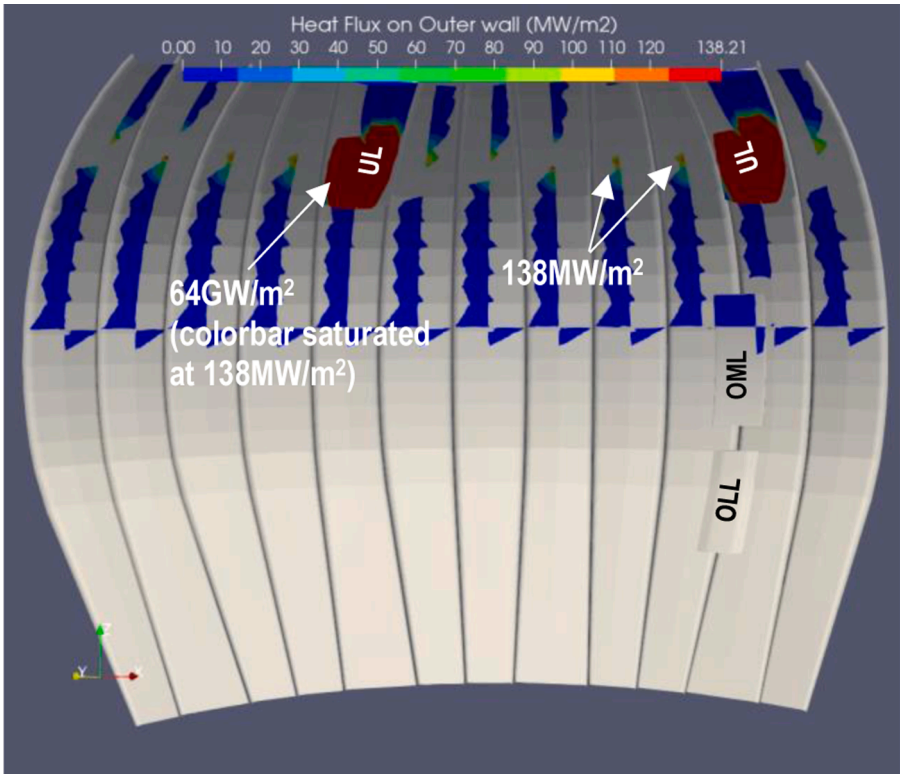

Fig. 10. HF for 4 ms during the U-VDE TQ using 8 UL and FW. The color bar is saturated at the value of the FW, i.e. 138 MW/m^2, as the UL peak value is 64 GW/m^2, for 4 ms.

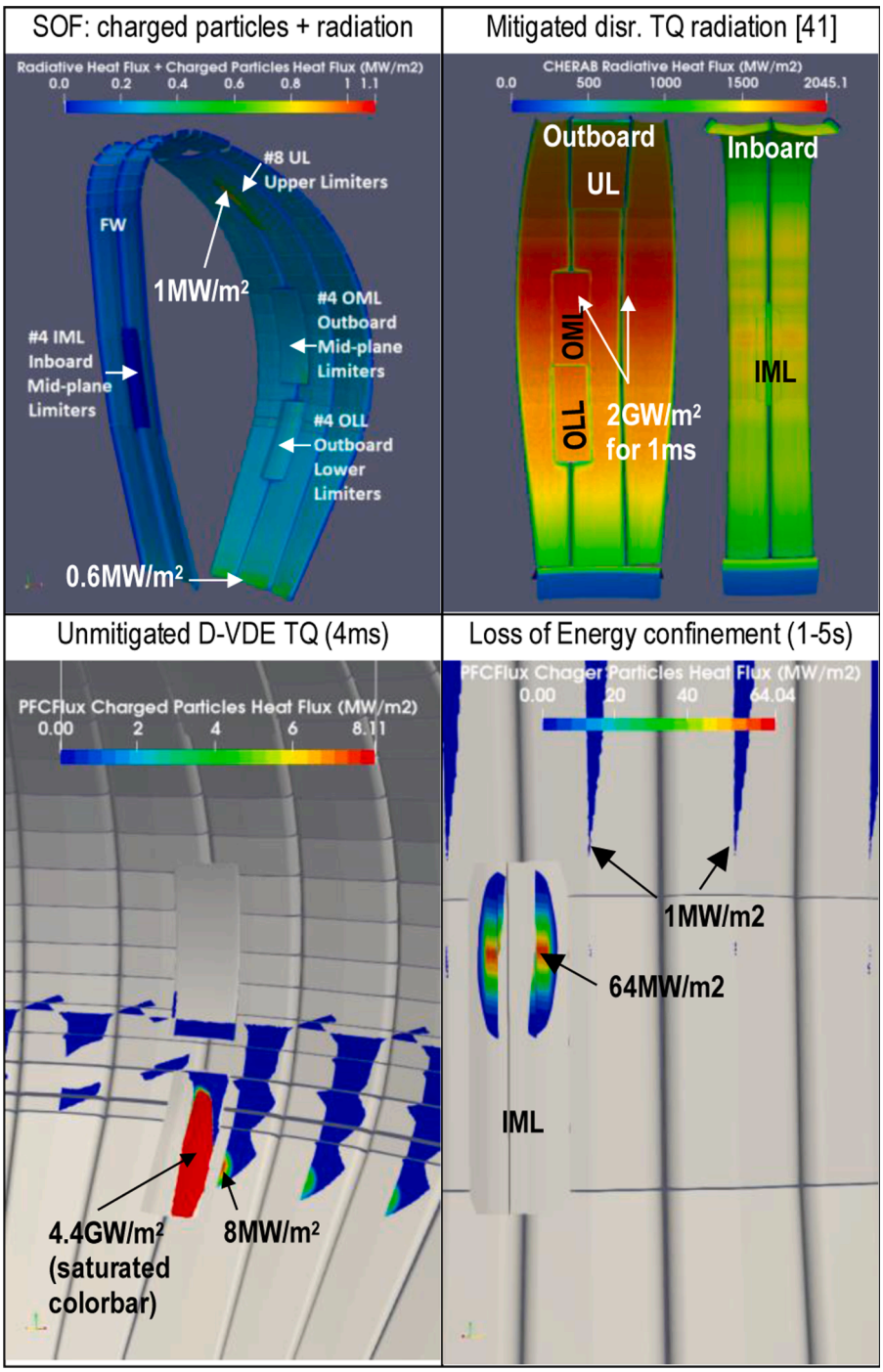

Fig. 11. Example of peak HF for steady state (SOF) and transient cases (i.e. Mitigated disruption, D-VDE and a conservative case of loss of confinement).

future simulations, with more combinations of perturbations and with added further 3D electromagnetic details, e.g. as ports. For this reason, it was decided to artificially shift the plasma boundary downward to touch such limiter, to scope out the maximum damage possible on such element, and the effectiveness in potentially protecting the FW and divertor system (although the latter was outside the scope of this KDII1). This will be revised in the future, as the need of the OLLs can be assessed with more accuracy.

For the "Loss of energy confinement" case, as stated in [10], it was also scoped out an intermediate TQ timescale, which at present does not correspond to any perturbation. This is because much faster transients would generally lead to an early TQ-CQ sequence leading to a U- or D-VDE before the plasma can touch the inner wall, and slower transients can be rejected by the shape control system. Also in this case, this was done to evaluate the effectiveness of IMLs in protecting the FW, and trigger integration studies. Early integration studies has proven to be very valuable, should a transient leading to a plasma-inner wall interaction be judged unavoidable in the future (e.g. even for technical reasons, such as a PF coil or power supply failure, or plasma overcooling due to many impurities). The assessment of the need of IMLs has been deferred to the CD Phase, hence many details are not at the same level of the other limiters. Finally, as it is possible to notice in Fig. 11 (bottom right), the surface shape of the IML presents a vertical grove, as described in details in [26], to allow the study of preliminary frontal remote maintenance concepts, as no ports are available in the inboard. This concept is similar to the inboard wall ITER FW panels [2, 42]. This

more complex shape leads to a higher HF load, up to 64MW/m^2, due to a smaller toroidal wetted area.

The 3D geometry developed was used, for all the most conservative cases described, to evaluate the HF on each PFC components. The details for the methodology used to calculate the photonic radiation loads during the mitigated disruption are described in [41, 43]. The Table 1 represents the collection of the heat load specifications on the FW and limiters for the different DEMO phases, and include links to the used inputs and produced output 3D data. This data is used as input by several EU-DEMO work packages (e.g. Divertor, Breeding Blanket, Balance of Plant) for detailed design and analysis activities.

A subset of critical instances, in the output columns of Table 1, is indicated with a superscript number within brackets, and was used to scope out the thermal behavior of the PFC, and to propose a simplified design. The results are commented in Section 6.

Aligning the limiters and the FW panels represents a significant challenge, which is mentioned also in [44]. A sensitivity study was performed by accounting for possible misalignments of the FW and limiters, due to technological limitations on fabrications, installations and different thermal expansion, in order to estimate the detrimental effects the PFC may experience. This work [45, 46] has been carried out within the activities related to this paper, and was preliminary performed on the normal operations SOF/EOF and RU. It eventually resulted in the calculation of penalty factor maps, which will be used as guideline to evaluate the peak heat fluxes, once more precise estimation of the misalignments will become available.

5.2. Single Null (SN) configuration with bare wall

The same SN described above, but with bare wall (without limiters), has been initially analysed, as one of the possible variants described in the introduction section, within the KDII1. The main results are hereafter summarised:

Assuming perfect alignment of the BB FW, it was found that the nominal HF in SOF and EOF operation due to DEMO charged particles and radiation does not exceed the BB FW capabilities. However, studies on the misalignments of the bare wall [47] have shown that, introducing preliminary misalignments of BB segments, up to +20mm, the steady-state HF are very close to the technological limits on 1-1.5MW/m^2, even in the nominal SOF/EOF cases, especially in the area close to the inactive secondary X-point.

For the nominal ramp-up/and down the maximum HF, even in the ideal case of perfectly aligned FW segments, is equal to 1.6 MW/m^2, above the standard FW-PFC limit, see Fig. 12. This was obtained for a plasma current of 2 MA, while we expect to transit from limited to diverted configuration between 3.5 MA and 6 MA, hence with an expected HF on the FW, respectively, from 1.75 to 3 times higher. Areas of the FW, close to the second X-point and the divertor baffles experience a HF of 1-1.5MW/m^2.

For the considered off-normal transients, leading to plasma-wall contact, extremely high heat fluxes, e.g. of the order of tens to hundreds of GW/m^2, were calculated for TQ phase following, respectively, the U/D-VDEs. This is in line with the order of magnitude evaluated for the sacrificial limiters surface, but such heat fluxes far exceed the BB FW capabilities causing severe damages to the thin W armour and down to the cooling pipe. This is true even with perfectly aligned FW segments, which would be challenging to achieve with the present ~9m tall BB back supporting structure [1]. An example is shown in Fig. 13 for the TQ phase of a D-VDE on the bare wall.

For these reasons, both the DEMO G1 review and the internal technical panels suggested to discard the variant of SN with the DEMO bare first wall.

6. Simplified thermal calculations analysis on DEMO PFC during plasma transients

The 3D HF calculations on the DEMO PFCs, reported in Table 1, have been used within this KDII1 to scope out the strategy of the FW protection from plasma transients. Starting from the broad range of results presented, a simplified analysis was carried out using the RACLETTE code [48] to quickly analyze the thermal behaviors of the specific PFC. Three main simplified designs were considered, according to the different functions and transients that the limiters are designed for:

First Wall. This is an input fixed from the present BB PFC designs, able to withstand up to 1-1.5MW/m^2 [1]. It includes: 2mm W armor, 2mm EUROFER heat sink, helium (He) coolant at ≈ 400°C, 80m/s velocity or water coolant (H_2O) at ≈ 300°C and 8m/s velocity. The H_2O model was preliminarily used, as it exhibits better performances.

RU/RD limiters (for the OML). During the RU normal operation, and possibly the RD, a maximum HF up to 2-3 MW/m^2 for tens of seconds is currently predicted. The DEMO W mono-block "Divertor like" solution is preliminary proposed including: 8 mm W armor, 2 mm CuCrZr pipe-heat

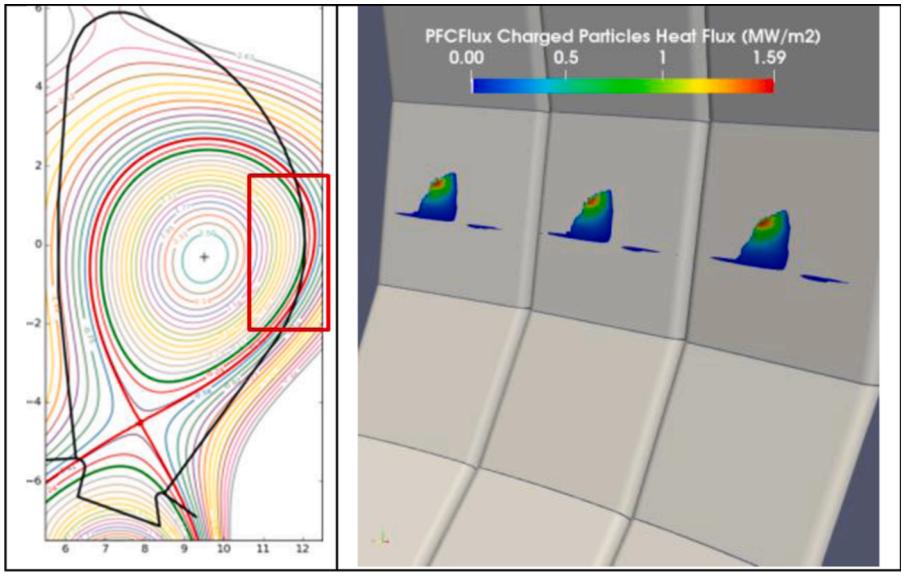

Fig. 12. Analysis of RU phases for the variant 1): SN without protection. Ideal case of perfectly aligned FW, and 2MA plasma current, results in a maximum HF equal to 1.6 MW/m^2.

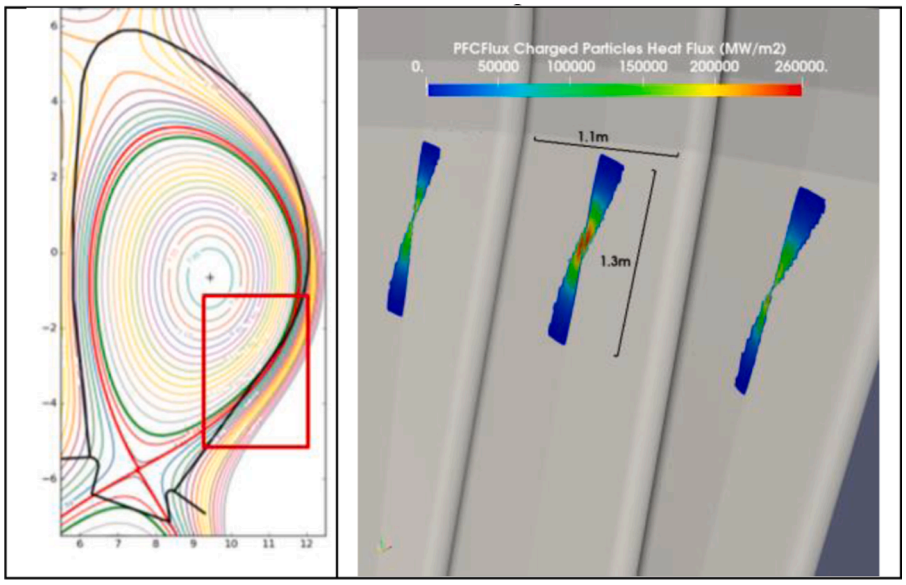

Fig. 13. Analysis of D-VDE phases for the variant 1): SN without protection. The maximum HF during the TQ is ≈ 260 GW/m^2 for 4ms, in an ideally perfectly aligned FW segments.

sink, water as coolant at ≈ 150°C temperature, and 8m/s velocity. This design can withstand steady state heat loads up to 10 MW/m^2, and hundreds of transients of tens of seconds up to 20 MW/m^2 [40]. As shown in the presented simulations in Fig. 5, this limiter shall not experience, by design, a direct contact with the plasma during off-normal events, as those intrinsically tend to be directed upward/-downward (due to the vertical instability of elongated plasma), or inboard (sudden loss of plasma energy).

Sacrificial Limiters (IML, UL, OLL): in contrast to RU/RD limiters, these protection limiters are designed for low power loads during normal operation and very high loads for very short times, during off-normal transients. The very preliminary design proposed, mainly for the initial thermal studies presented in this section, includes the same parameters as the divertor-like limiter, but with 20mm W armor. This design aims at taking advantage of the increased thermal capacity and reduced thermal conduction of the thick W. This is meant to protect the cooling pipe from reaching its limits. This condition may be achieved also with a thermal break like solution, as described in [26], or by using advanced W lattice materials [49, 50], see Section 6.2Section 6.2. These sacrificial limiters are meant to be far from the plasma, when the latter is in the nominal trajectory, as the minimum plasma-FW design clearance is by design of 22.5 cm at midplane, receiving relatively low HF. They are meant to be engaged directly by the plasma only for the off normal transients (e.g. mitigated/unmitigated disruptions, loss of energy confinement), when, as calculated in Table 1, they will be dealing with extremely high HFs (tens to hundreds of GW/m^2), for very short time ≤ 10-100ms. In these conditions, only the limiter W armor surface experiences a strong variation of temperature, which may reach the melting value of 3422°C, while the materials below remain almost unaffected. This design is proposed and analyzed for the UL, OLL and IML, which are designed to deal with off-normal events.

It needs to be mentioned that the evaluation of the limiter erosion has not been performed yet, and this may represent a direct source of W impurities for the plasma during the RU phase, which needs to be carefully accounted for. In Fig. 14, the three simplified PFC models used for the RACLETTE simulations are represented. The selected subset of critical cases, indicated in the Table 1 by a superscript number, were used as inputs to the code, by setting the HF density and the longest deposition time, and evaluating the thermal response. Four main outputs were extracted, as an update from the results presented in [10], and reported in Table 2, including: the W-armor vaporization and melting thickness (in μm), the armor surface (surf.) and the cooling pipe (acting as heat sink) temperature (in°C).

The maximum temperature considered for the cooling pipe, based on conservative criteria, was of 550°C for the EUROFER [51] and 350°C for the CuCrZr [52, 40].The main outcomes are:

For all cases analyzed, the FW is protected for all the envisaged transients, with no damages to the armor, nor the EUROFER. An

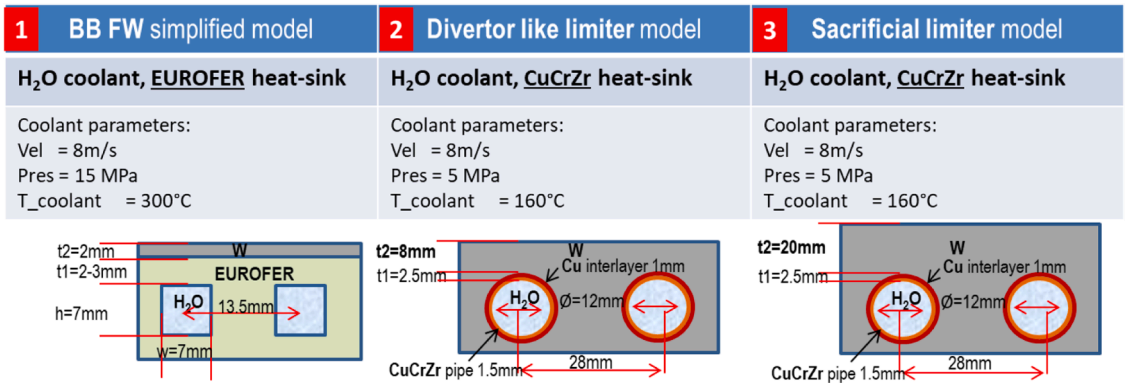

Fig. 14. Simplified PFC geometries and parameters used to scope out the plasma transient impact using the code RACLETTE.

Table 2
Results of simplified thermal analysis, run with the RACLETTE code, on different HF cases and PFC designs.

Case	W-vap. (μm)	W-Melt. (μm)	Surf. temp. (°C)	Pipe temp. (°C)
Divertor like limiter: (CuCrZr pipe/ heat sink lim. 350°C):				
D-VDE TQ [1]	0	0	958	171
Mitig. Dis. [11]	0	58	4676	168
Sacrificial limiter: (CuCrZr pipe/heat sink lim. 350°C):				
U-VDE FT [2]	0	0	1670	173
U-VDE TQ [3]	2770	1084	7921	169
D-VDE TQ [4]	Not converged			
H-L [5]	1040	4516	4729	280
H-L [6]	256	3869	4512	269
MD [7]	11	252	5674	168
Mitig. Dis. [11]	0	49	4437	168
First Wall (EUROFER heat sink temp. limit 550°C):				
U-VDE TQ [8]	0	0	958	383
D-VDE TQ [9]	0	0	1561	407
MD [10]	0	0	1765	415
Mitig. Dis. [11]	0	60	4676	429

exception is found for the conservative mitigated disruption, for which the peak photonic radiation needs to be reduced, with respect to the case considered, to avoid the melting of up to ~tens of μm. This is true for all the W-armor thicknesses of the 3 PFCs considered. This is mainly due to the toroidal and poloidal peaking factors, due to the discrete locations of the mitigation systems and the short release time for the radiation energy. This finding is applicable also for the ITER beryllium first wall [53], and recent modelling and experimental activity are being explored to mitigate these issues, e.g. in [54].

The discrete limiters guarantees that the cooling pipe is below the EUROFER and CuCrZr limits for all the 3 PFCs.

No damages are predicted for the RU/RD divertor-like limiters (OMLs) for any of the transients (except for the mitigated disruption case, mentioned above).

Severe damages are predicted for the sacrificial limiters armor (up to few mm), in case of unmitigated disruptions, while their cooling pipe remains always below the limits. This is true even for the conservative cases [5], [6] "Loss of energy confinement", arbitrarily chosen to cause plasma-IML contact.

For the other extreme case [4] D-VDE, artificially shifted downwards, the RACLETTE did not converge due to the extremely high W evaporation rate. For these cases, where the very fast armor vaporization plays an important role, the TOKES code [55] was employed instead, as reported in Section 6.1.

A broad range, in logarithmic steps, of constant heat flux densities, in MW/m^2, and deposition times, was used to produce maps of the thermal behaviors of the considered PFCs:

- Deposition time: from 1 ms to 10 s;
- Energy density: from 1 MJ/m^2 to 260 MJ/m^2.

The resulting maps are pictured in Fi. 15 for the sacrificial limiter model. In red and in brackets are indicated the cases from the Table 2.

These maps, produced also for the FW and "Divertor-like" PFC, can help to quickly estimate potential damages in case of future design, or assumption changes, and focus a more detailed analysis on a restricted

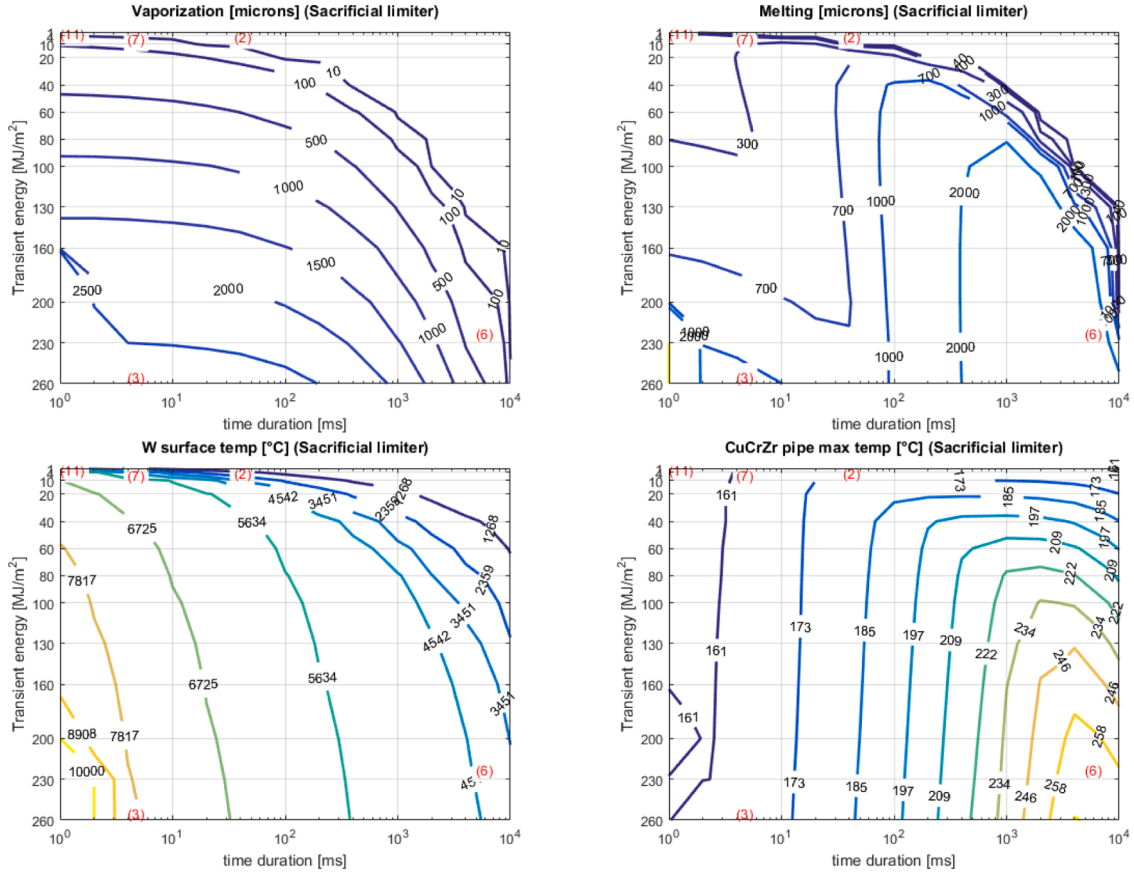

Fig. 15. Maps for the thermal behavior of the sacrificial limiters, produced with the RACLETTE code, including surface W- armor Vaporization, melting and temperature, and cooling pipe temperature, for a broad range of Energy densities and deposition times. In red parenthesis, are superimposed the most critical cases from Table 2.

number of cases of interest.

6.1. Preliminary studies on tungsten vapor shielding heat flux mitigation

Initial studies have been performed for the cases with extremely high HF, e.g. unmitigated disruption TQ, where the simplified thermal calculations are likely to be too conservative. For such cases, which lead to a large amount of W armor vaporization, potential benefits may arise from vapor shielding effects. The TOKES code [56], already used to simulate the vapor shielding in ITER divertor W mono-blocks and preliminary validated [57] on already existing data, was employed to simulate DEMO unmitigated TQ, following a MD [58] and a U-VDE [55], as shown in Fig. 16. The results, using for instance half of the total initial thermal energy (using the hypothesis that the other half is lost in the pre-TQ), show: for the U-VDE, an armor vaporization reduction from 35μm (without vapor shielding) down to 4μm (with vapor shielding) in the area where the UL is considered, and b) for the MD, a reduction from 150μm to 1μm for the DEMO divertor. More detailed results of the TOKES simulations are reported in [55, 58], while a model validation is presently being planned for the CDP, on ad-hoc experiments, within ITER and DEMO parameters and relevant diagnostics.

6.2. R&D for advanced solutions for the sacrificial limiter

In order to protect the sacrificial limiters cooling pipes and avoid a potential Loss Of Coolant Accident inside the DEMO chamber following a disruption, the thermal conduction of the materials surrounding the pipes can be suitably lowered. One approach that is being pursued to achieve this result includes the design and realization of models of advanced materials, such as W-lattice. These materials have a tailored design to obtain desired characteristics, and are realized in additive manufacturing. The desired properties being pursued are:

Less thermal stress/more ductility
Avoid heat sink overloading (low thermal conduction)
Hindered crack propagation
Prompt W vapor shielding

Samples have been designed [49], produced [59] (see Fig. 18), and are being tested [50], also in high HF test facilities Fig. 17. shows the cubic lattice samples of the W armour fabricated by the laser powder bed fusion technology. In this processing route, the lattice builds are 'printed' by selective laser melting of W power (either pure or doped with 6% Ta) and subsequent rapid cooling [60, 59]. This technology demonstrated a high flexibility in geometrical mapping from a CAD model for various design variants and a good production quality with acceptable costs Fig. 19. shows the optical microscopic images capturing the defects in the lattice ligaments. The defects comprise tiny pores and thin cracks introduced during the printing.

The major technology challenges are to reduce the defect density, to enhance microstructural homogeneity and to form a graded interlayer for joining dissimilar materials (e.g. W armour-to-steel heat sink) in a one-step printing process. Extensive preliminary tests were carried out to identify optimal processing parameters (e.g. laser power, beam scan speed, powder size, cooling temperature etc.). Mechanical tests (compressive) showed that the tungsten lattice samples had very low elastic stiffness in the range of 13-23MPa depending on the lattice architecture, which is roughly 5 orders of magnitude lower than the Young's modulus of tungsten (398GPa). The measured stiffness amounts only to 15-55% of the theoretical value (based on a FEM simulation). This discrepancy is attributed to the included defects. The low elastic stiffness may have the advantageous effect to reduce thermal stress and the effective thermal deformation [50]. The next step objectives will be 1) to develop a joining process for the tungsten-to-steel combination based on laser powder bed fusion, 2) to fabricate a small-scale joint mock-up with a water-cooled channel and 3) to verify the concept under transient extreme heat flux and long-pulse medium heat flux loads, respectively.

A second approach foresees the introduction of a thermal break [26] above the cooling pipe, using a concept similar to one of the options that have been explored for the DEMO divertor [40]. In this case, the low conductivity strip forces part of the heat load to the back of the heat sink, using it more efficiently also larger fraction of the W heat capacity. For both approaches, the reduced thermal conduction to the coolant brings, as a consequence, a higher armor surface temperature and, hence, a lower maximum steady HF capability. For this reason, they rely on the fact that the position of the sacrificial limiters (UL, IML and OLL) is, by design, far from the plasma nominal position, along all the pulse normal phases. Due to this design choice the sacrificial limiters have to withstand a lower steady state heat flux, e.g. with a maximum value of ~2.11 MW/m^2 for the IML during EOF, as visible on Table 1.

The higher surface temperature, if carefully tuned and if the consequence on the materials can be controlled, may be an advantage in promoting a prompter W-vaporization. As a consequence this will bring the possibility to enhance the radiation losses and vapor shielding effect in the off-normal cases, or during disruptions. These potential beneficial effects have to be carefully evaluated, but may bring to an additional layer of passive mitigation of PFC damages during disruptions.

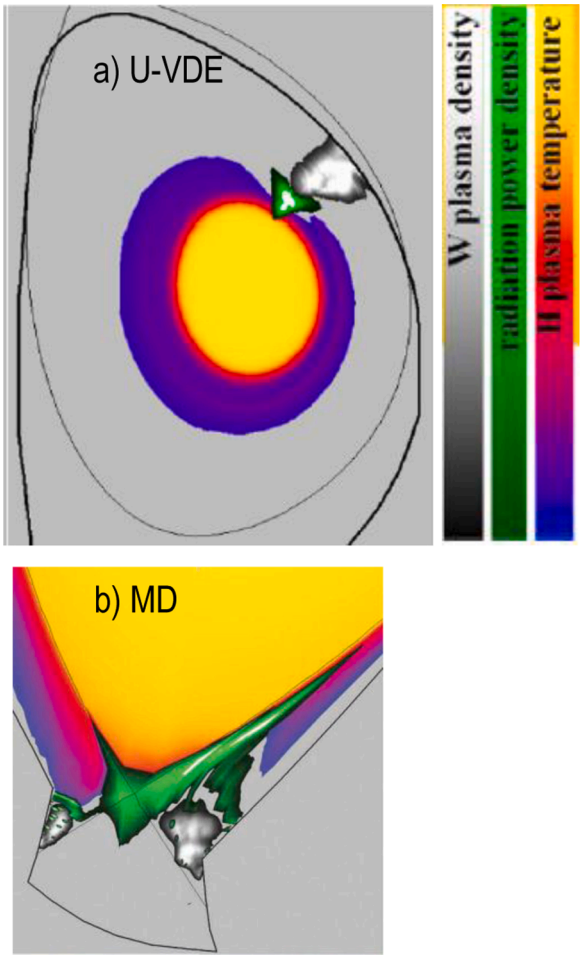

Fig. 16. TOKES simulation for a TQ during unmitigated disruption for: a) U-VDE [55], b) MD [58].

7. Limiter design

7.1. Functions and requirements

The main functions of the limiters are to sustain heat loads and to protect the BB FW from charged particles. The limiters must also provide neutron shielding to the VV and port plugs by absorption of neutrons.

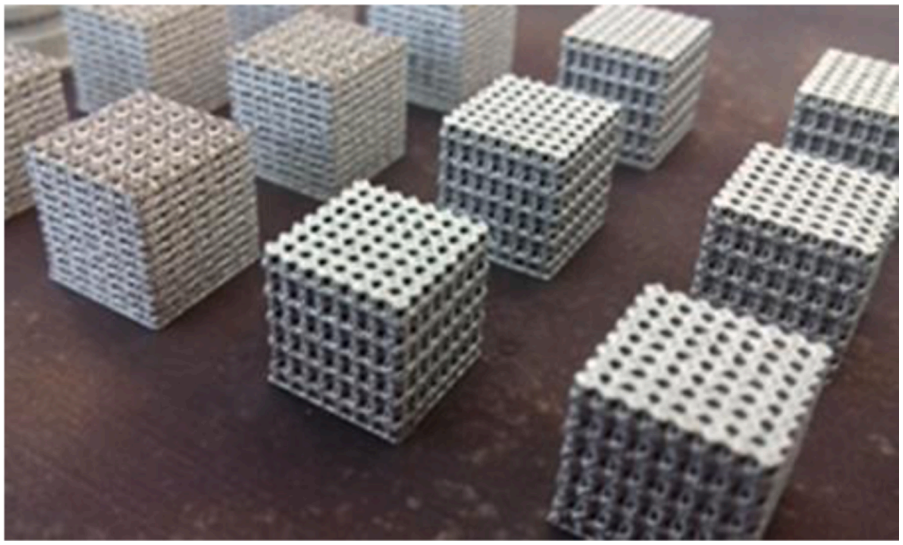

Fig. 17. Cubic lattice samples of the W armour fabricated by the laser powder bed fusion technology.

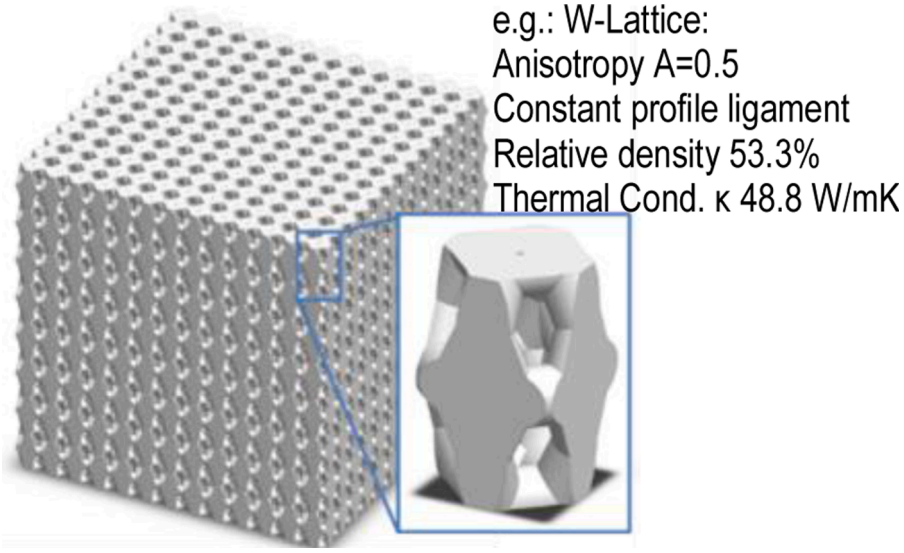

Fig. 18. Example of W-Lattice model, with desired material characteristics, e.g. designed with $\geq$ 50% of density, and $\leq$ 1/3 thermal conduction compared to the pure W.

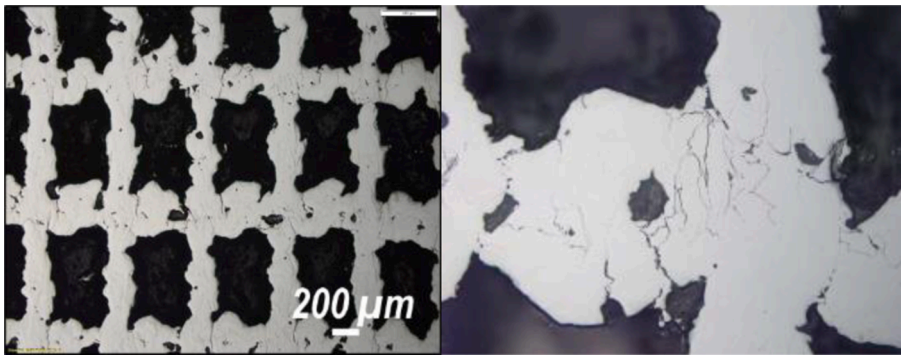

Fig. 19. Microscopic images of the laser-printed tungsten armour sample revealing defects in the lattice ligaments.

The significant heat must be removed by an active cooling system. A time and cost-efficient maintenance concept is required given the exposure of the PFCs to charged particles and significant neutron flux. This must be based on remote handling (RH) tools and should be facilitated by simple procedures for the installation of mechanical, electrical and service connections. The limiters should be integrated in such a way

that their replacement is not obstructed by the BB and hence not require the prior removal of any BB segments.

7.2. Design

Currently, the considered basic design of the limiters is, for the sake of simplicity, similar to that of the divertor [61]. The PFCs are based on copper alloys and have, depending on a specific function (e.g. sacrificial or "divertor-like RU" limiters), a relatively thick W armor, from 8mm to 20mm. The limiter plasma-facing surface is shaped in order to distribute impacting charged particles as evenly as possible during flat top operation and to avoid leading edges due to misalignments amongst the limiters [26, 45]. They are mounted on a water-cooled (for neutron moderation) steel structure named "shield block" that provides support and neutron shielding. It is made of the reduced activation steel EUROFER to minimize rad waste. Furthermore, the PFCs are water-cooled and, as in case of the divertor, two separate cooling loops are used for shield blocks and PFCs to allow the operation at different temperatures. This choice allows for the individual optimization of the cooling performance and the lifetime of the different materials under neutron irradiation [40, 62]. PFCs and shield blocks will be replaced together. All interfaces, e.g. to the cooling manifolds, will be integrated on the backside of the shield block.

7.3. Integration

The required locations of the plasma limiters are chosen in order to prevent the plasma from touching the BB FW in any transient events, see Fig. 20. As evaluated in Section 5, the following types of limiters are currently envisaged:

~8 upper limiters (ULs) [25]
~4 outboard mid-plane limiters (OMLs) [24]
~4 outboard lower limiters (OLLs), [3]
~4 inboard mid-plane limiters (IMLs) [26]

The limiters are integrated in the BB segments. To reduce the impact on the complex interior design of the BB segments and to maintain their vertical integrity, each UL replaces the upper part of a central outboard segment, whereas the OML, OLL and IML are integrated in-between two BB segments requiring slim rectangular cut-outs of two adjacent segments at a time, see Fig. 20. These cut-outs in the BB segments reduce the tritium-breeding ratio (TBR) the BB could achieve. This reduction was assessed recently and found roughly proportional to the total surface area of the limiters. The relative reduction of the TBR due to the integration of all currently considered limiters is ~8.0% for the helium-cooled pebble bed, and ~7.2% for the water-cooled lithium lead concept BB [63]. This is of significant impact on the tritium breeding function of the BB, especially by considering the additional loss of BB volume due to the integration of diagnostic and plasma heating systems, as well as the required excess production of tritium to compensate losses due to the natural tritium decay [3]. The actual number of limiter will have to be revised compatibly with the TBR requirements which depends on the type of blanket being considered [64].

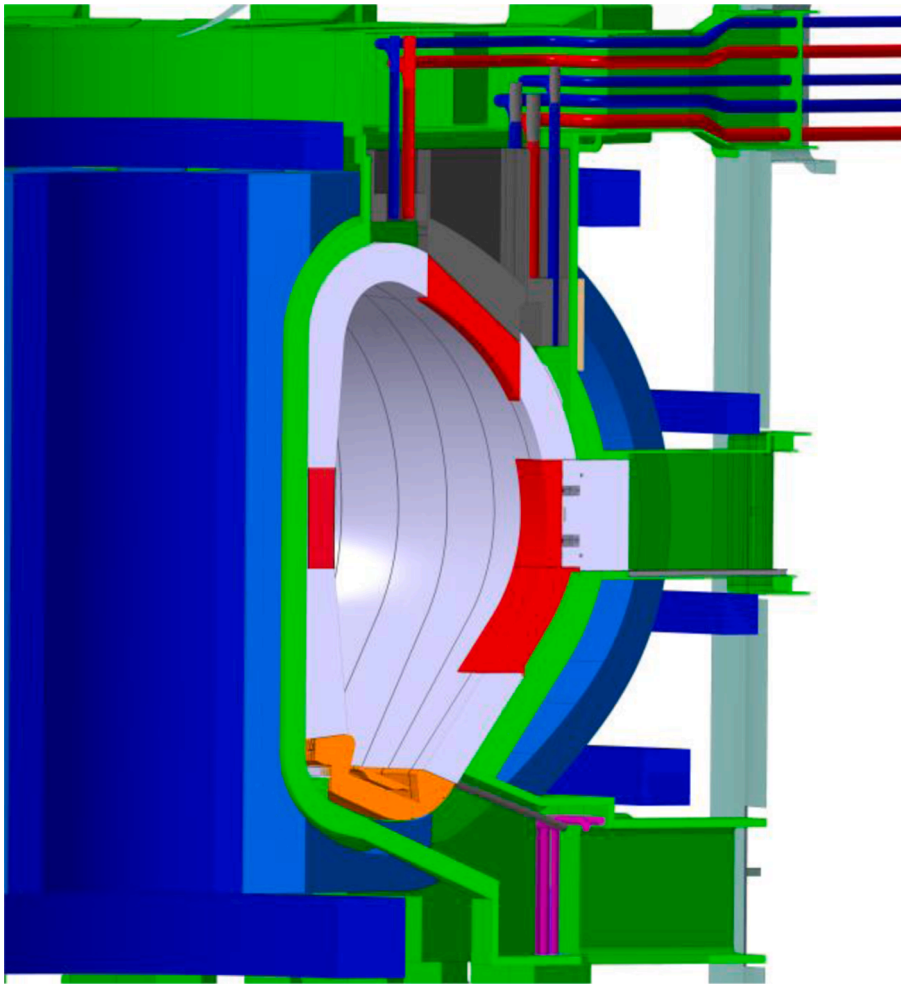

Fig. 20. DEMO poloidal cross-section with IMLs, ULs, OMLs, and OLLs (red), BB segments (grey), divertor (orange), and VV (green) [3].

7.4. Facilitation of remote replacement

The present preliminary design foresees that the ULs are replaced through the upper port, while the OMLs, OLLs, and IMLs are replaced through the equatorial ports. The pipes inside the ports are routed, where possible, outside the extraction paths of the limiters and mostly remain permanently inside the port. Short pipe stubs on the backside of a limiter shield block or a port plug are removed together with a limiter. Furthermore, the pipes do not penetrate the vacuum closure plates of the ports, see also [44]. Consequently, the access to the port closure plates is not obstructed, thus minimizing the required preparatory works for in-vessel maintenance. The OMLs and the ULs are integrated in port plugs and will be removed together with these. The corresponding RH tools can access the service and mechanical connections while the port plugs reduce the high gamma radiation of ~2100 Gy/h inside the plasma chamber to below 10 Gy/h inside the port cells [65]. Instead, the IMLs and the OLLs are directly attached to the VV. For their removal, the RH tools need to operate in the high dose environment. Due to the prior removal of the OMLs, the mechanical connections of the OLLs, as well as its cooling pipes, are well accessible. In case of the IMLs, both cooling pipes and mechanical connections might need to be accessed through the PFCs, much like in case of the ITER first wall and blanket [2]. Accessing the cooling pipes of the IMLs through the lower port has also been considered [26]. After removal from the VV at the end of their lifecycle, the shield blocks and PFCs are discarded as rad waste and replaced with new components. The port plugs instead are re-used since the neutron fluence lifetime is expected to be similarly low as that of the VV. These preliminary analyses and design efforts have been reviewed at the DEMO G1 meeting, and the main recommendation received is that the limiter maintenance scheme should be developed so as to allow the assessment of its impact on DEMO availability, which might be high. Some of the solutions proposed appear to be very challenging for IMLs and OLLs, which were developed with a lower level of details in the PCD Phase, for the reason stated above, and require further work. Furthermore, the DEMO technical internal panel remarked the need to provide an assessment of the implementation of the IMLs, by comparing the requirements from the plasma scenarios and from the induced effects and risks on the DEMO systems (TBR, neutron shielding, and maintenance).

8. Conclusions and future work

In this paper, it is presented an overview of the work done for the proposed strategy aimed at the protection of the EU-DEMO BB FW from plasma transients. This was part of the Key Design Integration Issue 1, presented at the DEMO G1, at the end of the PCD Phase. A design process was established to systematically evaluate the physics and engineering constraints, and list the steps that need to be taken to evaluate the effects that such steps have on the FW protection, also in case of change of assumptions or design choices. The G1 panel has recommended to put in place a more structured system engineering methodology for the CD Phase, in particular, to take into account predefined system requirements (e.g. erosion rates, maintenance constraints). Two variants were studied: SN without limiters (bare wall), and SN with discrete limiters. Some of the results, common for all the variants, are hereafter reported:

Mitigated disruptions: To stay within the melting limits of all the PFCs (FW and limiters) in the case of an ideally (in terms of radiated energy) mitigated disruption, a constraint needs to be prescribed on the maximum radiated power obtained by any possible mitigation system, e.g. by increasing the loss of energy in the pre-thermal quench, reducing the toroidal and poloidal peaking factors.

Major (Centered) Disruptions: The limiters do not protect the divertor in case of a central disruption.

The main results for each variant are instead hereafter reported.

8.1. Variant SN with bare wall

This configuration was judged "not viable" in neither nominal transient phase, such as RU and RD, nor in off-normal events (e.g. U/D-VDE, MD), as the heat flux to the FW, even in the ideally aligned blanket segment case, is above the PFC capability of ≈1-2MW.

8.2. Variant SN with discrete limiters

Discrete limiters are proposed to protect the BB FW from plasma transients and, so far, seem to represent a viable solution, as no show-stoppers have been found. These limiters shall be replaceable through the VV ports without the need of prior removal of the BB or divertor. Two different PFCs are envisaged:

"DEMO divertor-like" limiters, capable of exhausting up to few tens of MW/m^2 for few tens of s, for RU, and possible RD phases sacrificial limiters, for off-normal transients, able to sustain loads ranging from hundreds of MW/m^2 to tens of GW/m^2 for times up to few tens of ms. A tentative proposed design could foresee a divertor like PFC with a thicker W armor (up to 20 mm)

It is considered preferable to integrate sacrificial limiters as far as possible from the plasma, in order for them to be engaged only in the off-normal events, which must be very rare. This is because they have a lower maximum steady state HF capability, and a protection limiter with a slightly damaged surface may still maintain its function to protect the FW. The evaluated heat loads included the charged particles and the photonic radiation, and have been summarised in Table 1. The main findings are:

Simplified thermal analysis using the RACLETTE [48] code have shown that damage to the BB FW is prevented in all considered transients.

For all the considered normal and off-normal plasma phases, the cooling channels of the FW and all the limiters, are within the limits, respectively of 550C (for EUROFER) and 350C (for CuCrZr).

The heat loads on the ramp-up limiters (i.e., OMLs) were found to be within the limits. E.g. by making the hypothesis of using a "divertor like" W monoblock solution.

In the most extreme cases, e.g. during unmitigated disruption TQ, severe damages are expected on the protection limiters (ULs, OLLs) armor surface, with up to 1 mm-deep melting, or up to 4.5 mm in case of conservative "Loss of confinement energy" transition on the IMLs, out of the total 20 mm of the design proposed. For these extreme cases possible mitigation effects coming from the W vapor shielding were modelled [58, 55], as described in Section 6.1, and are presently being assessed on experimental devices, similarly to ITER [57].

At present, conservative assumptions are made for the "Loss of confinement energy" and "D-VDE" transients, artificially inducing plasma-PFC contact. This was done to scope which size and toroidal number of limiters would be needed to protect the FW. These hypotheses will be reviewed in the CD Phase, as the possibility to avoid the presence of the IML and OLL will greatly simplify the design and the maintenance of the in-vessel components.

Studies on the damages due to runaway electrons (REs) are in a very preliminary phase. As this area represents a well-recognized problem, DEMO design could benefit from possible ITER solutions [66]. A fully consistent closed loop simulation of the plasma transients, including strongly coupled magnetic and kinetic control, named is currently being developed. The delivery of this tool, named "Flight simulator", represents one of the main objective of the next Conceptual Design Phase.

CRediT authorship contribution statement

Francesco Maviglia: Conceptualization, Methodology, Formal analysis, Writing – original draft, Writing – review & editing, Visualization, Supervision, Project administration. **Christian Bachmann:** Conceptualization, Methodology, Validation. **Gianfranco Federici:**

Methodology, Funding acquisition, Supervision. **Thomas Franke:** Methodology. **Mattia Siccinio:** Methodology, Conceptualization. **Raffaele Albanese:** Methodology, Software, Investigation. **Roberto Ambrosino:** Methodology, Software, Investigation. **Wayne Arter:** Software. **Roberto Bonifetto:** Software, Validation. **Giuseppe Calabrò:** Supervision. **Riccardo De Luca:** Software, Investigation, Validation. **Luigi E. Di Grazia:** Software. **Emiliano Fable:** Methodology, Software, Investigation, Validation. **Pierluigi Fanelli:** Methodology, Software, Investigation. **Alessandra Fanni:** Supervision. **Mehdi Firdaouss:** Methodology, Software. **Jonathan Gerardin:** Methodology, Software, Investigation, Validation, Data curation, Visualization. **Riccardo Lombroni:** Methodology, Software. **Massimiliano Mattei:** Methodology, Software, Investigation. **Matteo Moscheni:** Methodology, Software, Investigation, Validation. **William Morris:** Conceptualization. **Gabriella Pautasso:** Conceptualization. **Sergey Pestchanyi:** Methodology, Software, Investigation, Validation. **Giuseppe Ramogida:** Software. **Maria Lorena Richiusa:** Methodology, Software, Investigation, Validation. **Giuliana Sias:** Methodology, Software, Investigation. **Fabio Subba:** Investigation, Validation. **Fabio Villone:** Methodology, Software, Investigation. **Jeong-Ha You:** Supervision. **Zsolt Vizvary:** Methodology, Software, Investigation.

Declaration of Competing Interest

The authors declare that they have no known competing financial interests or personal relationships that could have appeared to influence the work reported in this paper.

Acknowledgments

The authors would like to thank Dr. Andre Grosman as representative of the DEMO Technical Advisory Group (TAG), and the other members of the TAG, for their thorough review of the work presented in this paper, and at the 2020 G1 gate review. This work has been carried out within the framework of the EUROfusion Consortium and has received funding from the Euratom research and training programme 2014-2018 and 2019-2020 under grant agreement No 633053. The views and opinions expressed herein do not necessarily reflect those of the European Commission.

References

[1] F. Cismondi, et al., Progress in EU Breeding Blanket design and integration, FED 136 (2018) 782–792, https://doi.org/10.1016/j.fusengdes.2018.04.009.
[2] A.R. Raffray, et al., The ITER blanket system design challenge, Nucl. Fusion 54 (2014), 033004.
[3] C. Bachmann, et al., Key design integration issues addressed in the EU DEMO pre-concept design phase, Fus. Eng. Des. (2020).
[4] G. Federici, et al., DEMO design activity in Europe: Progress and updates, FED (2018).
[5] M. Siccinio, et al., Development of the plasma scenario for EU-DEMO: status and plans, FED (2022), https://doi.org/10.1016/j.fusengdes.2022.113047 this issue.
[6] M. Siccinio, et al., Impact of the plasma operation on the technical requirements in EU-DEMO, FED (2022) this issue.
[7] R. Pitts, et al., Heat and Nuclear Load Specifications, (ITER internal report v2.3, idm_2LULDH) (2022).
[8] G.V. Pereverzev, et al., ASTRA - Automated System for TRansport Analysis," Max-Planck-Institut Für Plasmaphysik,, IPP-Rep. (2002). IPP 5/98.
[9] X. Bonnin, et al., Presentation of the New SOLPS-ITER Code Package for Tokamak Plasma Edge Modelling, Plasma Fusion Res. 11 (2016), 1403102.
[10] F. Maviglia, et al., Impact of plasma thermal transients on the design of the EU DEMO first wall, Fus. Eng. Des. (2020), https://doi.org/10.1016/j.fusengdes.2020.111713.
[11] R. Wenninger, et al., The DEMO wall load challenge, Nucl. Fusion 57 (2017), 046002, https://doi.org/10.1088/1741-4326/aa4fb4.
[12] F. Maviglia, et al., Optimization of DEMO geometry and disruption location prediction, FED 146 (2019) 967–971, https://doi.org/10.1016/j.fusengdes.2019.01.127.
[13] G. Maddaluno, et al., "Wall loads during disruptions (EUROfusion internal report)," 2018.
[14] R. Albanese, et al., CREATE-NL+: A robust control-oriented free boundary dynamic plasma equilibrium solver, FED (2015).
[15] P. Barabaschi, "The MAXFEA code," in ITER EDA Plasma Control Technical Meeting, Naka, Japan (1993).
[16] R. Albanese, et al.,, "Numerical Studies of the Next European Torus via the PROTEUS Code," 12th Conference on the Numerical Simulation of Plasmas, S. Francisco,, Sept. 1987 .
[17] F. Villone, et al., Coupling of nonlinear axisymmetric plasma evolution with three-dimensional volumetric conductors, PPCF (2013).
[18] R. Lombroni, et al., Using MAXFEA code in combination with ANSYS APDL for the simulation of plasma disruption events on EU DEMO, Fus. Eng. Des 170 (2021), https://doi.org/10.1016/j.fusengdes.2021.112697 p. In Press.
[19] G. Sias, et al., Inter-machine plasma perturbation studies in EU-DEMO relevant scenarios: lessons learnt for EM forces prediction during VDEs, Nuclear Fusion (2022). https://doi.org/10.1088/1741-4326/ac53c1.
[20] F. Maviglia, et al., Impact of plasma-wall interaction and exhaust on the EU-DEMO design, Nuclear Mater. Energy (2021), https://doi.org/10.1016/j.nme.2020.100897.
[21] L. Lao, "G EQDSK FORMAT," 1997.
[22] F. Villone, et al., Neutral point detection in JET, FED (2003), 709/714.
[23] R. Albanese, et al.,, "2D- Vertical Stability (VS) analysis," (EUROfusion internal report idm_2N2CGV), 2017.
[24] T. Franke, et al., The EU DEMO equatorial outboard limiter - design and port integration concept, Fus. Eng. Des (2020).
[25] C. Vorpahl, et al., Initial configuration studies of the upper vertical port of the European DEMO, Fus. Eng. Des (2019).
[26] Z. Vizvary, et al., European DEMO first wall shaping and limiters design and analysis status, Fus. Eng. Des. (2020).
[27] P. Pereslavtsev, et al., Neutronic analyses for the optimization of the advanced HCPB breeder blanket design for DEMO, Fus. Eng. Des (2017).
[28] M. Carr, et al., Towards integrated data analysis of divertor diagnostics with ray-tracing, in: 44th EPS Conference on Plasma Physics, 2017.
[29] M. Firdaouss, et al., Modelling of power deposition on the JET ITER like wall using the code PFCFlux, J. Nucl. Mater. 348 (2013) 536.
[30] W. Arter, et al., The SMARDDA approach to ray-tracing and particle tracking, IEEE Trans. Plasma Sci. (2015) 3323. Vols43-9.
[31] J. Gerardin, et al., "Simplified heat load modelling for design of DEMO discrete limiter," Nuclear Materials and Energy, Vols. 20, pp.100568, 2019.
[32] R. Mitteau, Private communications..
[33] M. Kobayashi, et al.,, "3D edge transport analysis of ITER start-up configuration for limiter power load assessment," 2007.
[34] "https://vtk.org/".
[35] C. Silva, et al., Characterization of scrape-off layer transport in JET limiter plasmas, Nucl. Fusion (2014).
[36] P.C. Stangeby, R. Mitteau, Analysis for shaping the ITER First Wall, J. Nuclear Mater. (2009).
[37] F. Maviglia, et al., Effect of engineering constraints on charged particle wall heat loads in DEMO, FED (2017), https://doi.org/10.1016/j.fusengdes.2017.02.077.
[38] F. Maviglia, et al., Wall protection strategies for DEMO plasma transients, Fus. Eng. Des. (2018), https://doi.org/10.1016/j.fusengdes.2018.02.064.
[39] R.A. Pitts, et al., Physics basis and design of the ITER plasma-facing components, JNM (2011).
[40] J.H. You, et al., Conceptual design studies for the European DEMO divertor: Rationale and first results, Fus. Eng. Des. (2016).
[41] M. Moscheni, et al., Radiative heat load distribution on the EU-DEMO first wall due to mitigated disruptions, Nucl. Mater. Energy 25 (2020), 100824.
[42] R. Mitteau, et al., The design of the ITER first wall panels, Fus. Eng. Des. (2013).
[43] M. Moscheni, et al., Parametric study of the radiative load distribution on the EU-DEMO first wall due to SPI-mitigated disruptions, Fus. Eng. Des. (2021).
[44] C. Bachmann, et al., Containment structures and port configurations, Fus. Eng Des. (2022), https://doi.org/10.1016/j.fusengdes.2021.112966 this issue.
[45] M.L. Richiusa, et al., Poloidal distribution of penalty factors for DEMO Single Module Segment with limiters in normal operation, Fus. Eng. Des. (2021).
[46] D.C. Calleja, et al., Strategy for Sensitivity Analysis of DEMO first wall, in: 3rd International Conference on Vulnerability and Risk Analysis and Management (ICVRAM), 2018.
[47] Z. Vizvary, et al., DEMO First Wall misalignment study, Fus. Eng. Des. (2019), https://doi.org/10.1016/j.fusengdes.2019.04.046 no.
[48] A.R. Raffray, et al., RACLETTE: A model for evaluating the thermal response of plasma facing components to slow high power plasma transients. Part I: Theory and description of model capabilities, J. Nucl. Mater. 244 (1997) 85–100.
[49] R.De Luca, et al., Preliminary investigation on W foams as protection strategy for advanced FW PFCs, Fus. Eng. Des. (2019).
[50] R.De Luca, et al., Comparison between finite element and experimental evidences of innovative W lattice materials for sacrificial limiter applications, Fus. Eng. Des. (2021).
[51] F. Arbeiter, et al., Thermal-hydraulics of helium cooled First Wall channels and scoping investigations on performance improvement by application of ribs and mixing devices, FED (2016) 1123–1129. Vols. 109-111.
[52] M. Miskiewicz, et al., Impact of plastic softening of over-aged CuCrZr alloyheat sink tube on the structural reliability of a plasma-facing component, FED (2008).
[53] I. Landman, et al., Radiation loads on the ITER first wall during massive gas injection, Fus. Eng. Des. (2013).
[54] S. Park, Experimental results of multiple shattered pellet injection systems in KSTAR, Fus. Eng. Des. (2021).
[55] S. Pestchanyi, et al., Simulation of the first wall shielding during upward VDE in DEMO, Nucl. Mater. Energy (2020).

[56] S. Pestchanyi, et al., Simulation of divertor targets shielding during transients in ITER, FED (2016).
[57] S. Pestchanyi, et al., Validation of TOKES vapor shield simulations against experiments in the 2MK-200 facility, Fus. Eng. Des. (2017).
[58] S. Pestchanyi, et al., Simulation of the Divertor Target Shielding During Major Disruption in DEMO, Fusion Sci. Technol. (2019).
[59] A.v. Müller, et al., Tailored tungsten lattice structures for plasma-facing components in magnetic confinement fusion devices, Mater. Today (2020).
[60] N. Mantel, et al., Development and testing of an additively manufactured lattice for DEMO limiters, Nucl. Fusion (submitted) (2022).
[61] G. Mazzone, et al., Eurofusion-DEMO Divertor - Cassette Design and Integration, FED (2020).
[62] G. Mazzone, et al., Choice of a low operating temperature for the DEMO EUROFER97 divertor cassette, Fus. Eng. Des. (2017).
[63] P. Pereslavtsev, et al., DEMO tritium breeding performances with different in-vessel components configurations, Fus. Eng. Des. (2021), 166 112319.
[64] U. Fischer, et al., Methodological approach for DEMO neutronics in the European PPPTprogramme: Tools, data and analyses, Fus. Eng. Des. (2017), 123 26-31.
[65] D. Leichtle, et al., Global shutdown dose rate maps for a DEMO conceptual design, Fus. Eng. Des. (2015).
[66] R. Pitts, et al., Physics basis for the first ITER tungsten divertor, Nucl. Mater. Energy (2019).